Pergamon

Atmospheric Environment Vol. 29, No. 21, pp. 2929–2960, 1995

1352-2310/95 $9.50 + 0.00

1352-2310(95)00113-1

DEVELOPMENT AND TESTING OF METEOROLOGY AND AIR DISPERSION MODELS FOR MEXICO CITY

M. D. WILLIAMS,* M. J. BROWN,* X. CRUZ,† G. SOSA† and G. STREIT*

* Los Alamos National Laboratory, Mail Stop B299, Los Alamos, NM 87545, U.S.A.; and † Instituto Mexicano del Petróleo, Gerencia de Energéticos Alternos y Quimica Ambiental, Apdo. Postal 14-805, México, D.F. 07730, Mexico

(*First received* 1 *November* 1993 *and in final form* 16 *January* 1995)

Abstract—Los Alamos National Laboratory and Instituto Mexicano del Petróleo are completing a joint study of options for improving air quality in Mexico City. We have modified a three-dimensional, prognostic, higher-order turbulence model for atmospheric circulation (HOTMAC) and a Monte Carlo dispersion and transport model (RAPTAD) to treat domains that include an urbanized area. We used the meteorological model to drive models which describe the photochemistry and air transport and dispersion. The photochemistry modeling is described in a separate paper. We tested the model against routine measurements and those of a major field program. During the field program, measurements included: (1) lidar measurements of aerosol transport and dispersion, (2) aircraft measurements of winds, turbulence, and chemical species aloft, (3) aircraft measurements of skin temperatures, and (4) Tethersonde measurements of winds and ozone. We modified the meteorological model to include provisions for time-varying synoptic-scale winds, adjustments for local wind effects, and detailed surface-coverage descriptions. We developed a new method to define mixing-layer heights based on model outputs. The meteorology and dispersion models were able to provide reasonable representations of the measurements and to define the sources of some of the major uncertainties in the model–measurement comparisons.

Key word index: Prognostic models, complex terrain, urban air quality, measurement–model comparison, Mexico City.

1. INTRODUCTION

Mexico City has a serious air pollution problem. For example, ozone (O_3) levels exceeded Mexican air quality standards on approximately 350 d in 1992. The highest O_3 levels are approximately 0.4 ppm, a value that is significantly higher than found in Los Angeles in recent years. Mexico City's large population (~20 million) and topography are important contributors to the air pollution problem. Mexico City lies at an elevation of approximately 2200 m (7500 ft) above sea level in a "U" shaped basin that opens to the North. Mountains on the east and southeast sides of the basin form a barrier with a height of approximately 3700 m (12,000 ft), while two isolated peaks reach elevations in excess of 5300 m (17,400 ft). The city occupies a major part of the southwest portion of the basin. During the wintertime when the worst air quality episodes occur, the winds are frequently light and out of the northeast. Although the winds are light within the city, significant slope winds develop which influence the behavior of the pollutants. The result of this combination of circumstances is a relatively short residence time for morning rush-hour emissions, but a long residence time for afternoon and evening emissions.

Los Alamos National Laboratory and Instituto Mexicano del Petróleo are completing a joint study of options for improving air quality in Mexico City. The U.S. Department of Energy supported the efforts of the Los Alamos investigators, while PEMEX supported the efforts of the Mexican researchers. The task of developing a comprehensive air quality modeling system for any major city is a difficult one. In order to develop a good understanding of urban air quality in major cities, three major components are needed: (1) measurements, (2) emission inventories, and (3) air quality models. Despite many years of development, none of the components can be considered perfect. Measurements may be accurate, but they may not be representative of what we should know for

understanding the air quality situation and for modeling air quality changes (e.g. Thomson, 1986). Emission inventories represent areas of major uncertainties (e.g. Gertler and Pierson, 1991; Oliver *et al.*, 1993). In cities where there has been considerable work over many years, it appears that the emissions inventories are inconsistent with ambient measurements. Air quality models have had both successes and failures (e.g. Wilson, 1993).

Many of these concerns are enhanced in an application to Mexico City, where the measurements are limited and the emissions have not been investigated as thoroughly. The routine measurements in the Mexico City area are primarily located within the city itself and are taken near the surface. Upper-level winds are provided by rawinsondes at the airport, while low-level winds are measured at several sites within the city. Many of the sites have obstructed upwind fetches for several directions. The focus of the pollution monitoring, carried out by the Secretaría de Desarollo Social (SEDESOL), has been on the pollutants of health-related concern, such as carbon monoxide (CO), ozone (O_3), and sulfur dioxide (SO_2). This monitoring is quite appropriate if one wants to know what the current air quality is, but it tells us little about the levels of hydrocarbons (HC) and oxides of nitrogen (NO_x), the building blocks for O_3. Typically, there are only five stations monitoring NO_x and two monitoring nonmethane hydrocarbons. Furthermore, there is no routine monitoring of hydrocarbon speciation and hydrocarbon speciation is very important to O_3 formation.

In this paper, we address the meteorological and air dispersion modeling aspects of the study (separate papers address the photochemical modeling and the additional measurements we made). We have used the sophisticated higher-order turbulence closure model for atmospheric circulation (HOTMAC model) to overcome the complexity of the terrain and the relative paucity of meteorological data. The use of the random particle transport and dispersion (RAPTAD) model eliminated many of the limitations inherent in Gaussian-type air quality models (e.g. the latter cannot readily handle unsteady conditions, complex terrain, and wind shear). We have made direct comparisons between modeled and measured meteorological and concentration variables and we have also calculated a variety of statistical parameters for evaluating the comparisons.

2. THE METEOROLOGICAL MODELING SYSTEM

The objective of the meteorological modeling was to provide atmospheric transport variables for the dispersion and air chemistry models, and to help provide an understanding of the air quality situation. For major urban areas there are two approaches to defining transport variables. One involves interpolating between measurements to provide winds at all points of interest. The other approach involves modeling winds with a meteorological model that can compute a full, three-dimensional time-dependent wind field. The intent of the latter approach, which we used, is to represent the important physics in detail rather than relying on a dense system of measurements to provide the physics from the measurements alone.

2.1. *Model formulation*

HOTMAC is a three-dimensional time-dependent model (Yamada and Bunker, 1988). It uses the hydrostatic approximation and a terrain-following coordinate system. HOTMAC solves conservation equations for the horizontal wind components, potential temperature, moisture, turbulent kinetic energy, and the turbulence length scale. HOTMAC describes advection, Coriolis effects, and turbulent transfer of heat, momentum, and moisture. It also describes solar and terrestrial radiation effects, turbulent history effects, and the drag and radiation effects of forest canopies. The lower boundary conditions are defined by a surface energy balance and similarity theory. The local soil heat flux is obtained by solving a soil heat conduction equation that ignores horizontal heat transfer. In an urban context the surface energy balance requires an additional term that represents the heat released by man's activities. The additional heat, along with differences in thermal and albedo properties between urban and nonurban surfaces, produces the urban heat island.

We used a nested grid system to model the valley of Mexico and its surrounding terrain. The outer grid is a 20 by 25 array of cells and has a 6 km spacing and covers the major terrain influences as shown in Fig. 1. The inner grid which has a 21 by 27 array of cells is depicted as a box within the outer grid and it embraces the city and its immediately adjacent slopes. The inner grid has a resolution of 2 km. The individual characters plotted on the figure are monitoring sites operated by SEDESOL. The area in yellow represents the urban area as defined by estimated CO emissions. The mountainous area in the North central part of the inner grid is Pico de Tres Padres which plays an important role in some circumstances.

2.2. *Model development*

At the start of this project, HOTMAC used two major sets of inputs: only a single vertical profile of winds, temperatures, and relative humidity and simplified topography (i.e. either land or water). The meteorological profiles were used to describe the synoptic (large-scale) conditions of winds, temperatures, and moisture and did not vary with time. The model was initialized with the potential temperature assumed to be the same in every location for any given height above mean sea level. The large-scale winds were derived from the winds used to initialize the model. Essentially, a single wind speed and direction aloft were used to produce the effects of the large-scale

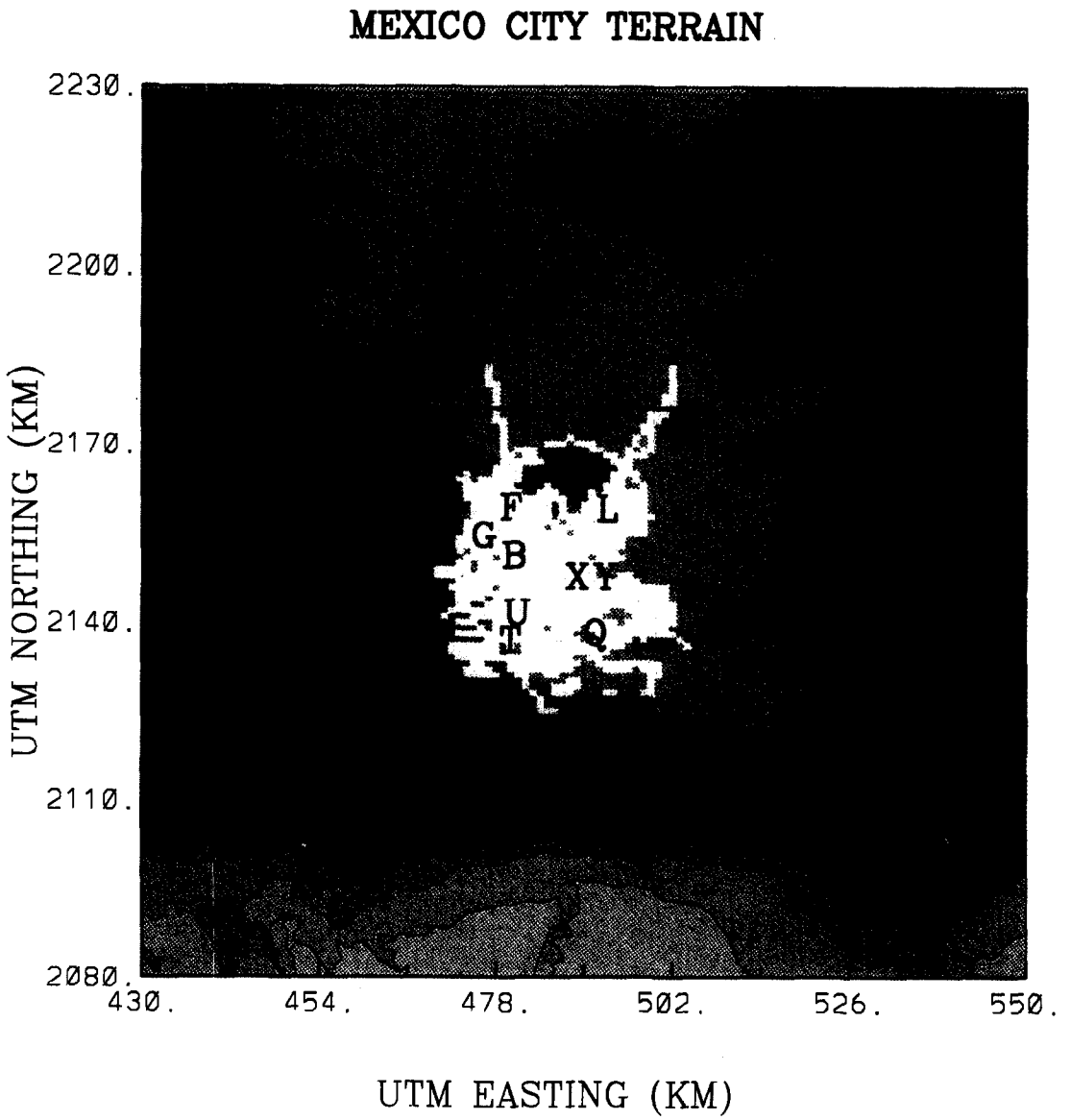

Fig. 1. Model domains for the Mexico City air basin. The beige area represents an approximate elevation range from 1000 to 1460 m msl, while the white area at the top of the volcanoes represents an approximate range of 4140–4600 m msl.

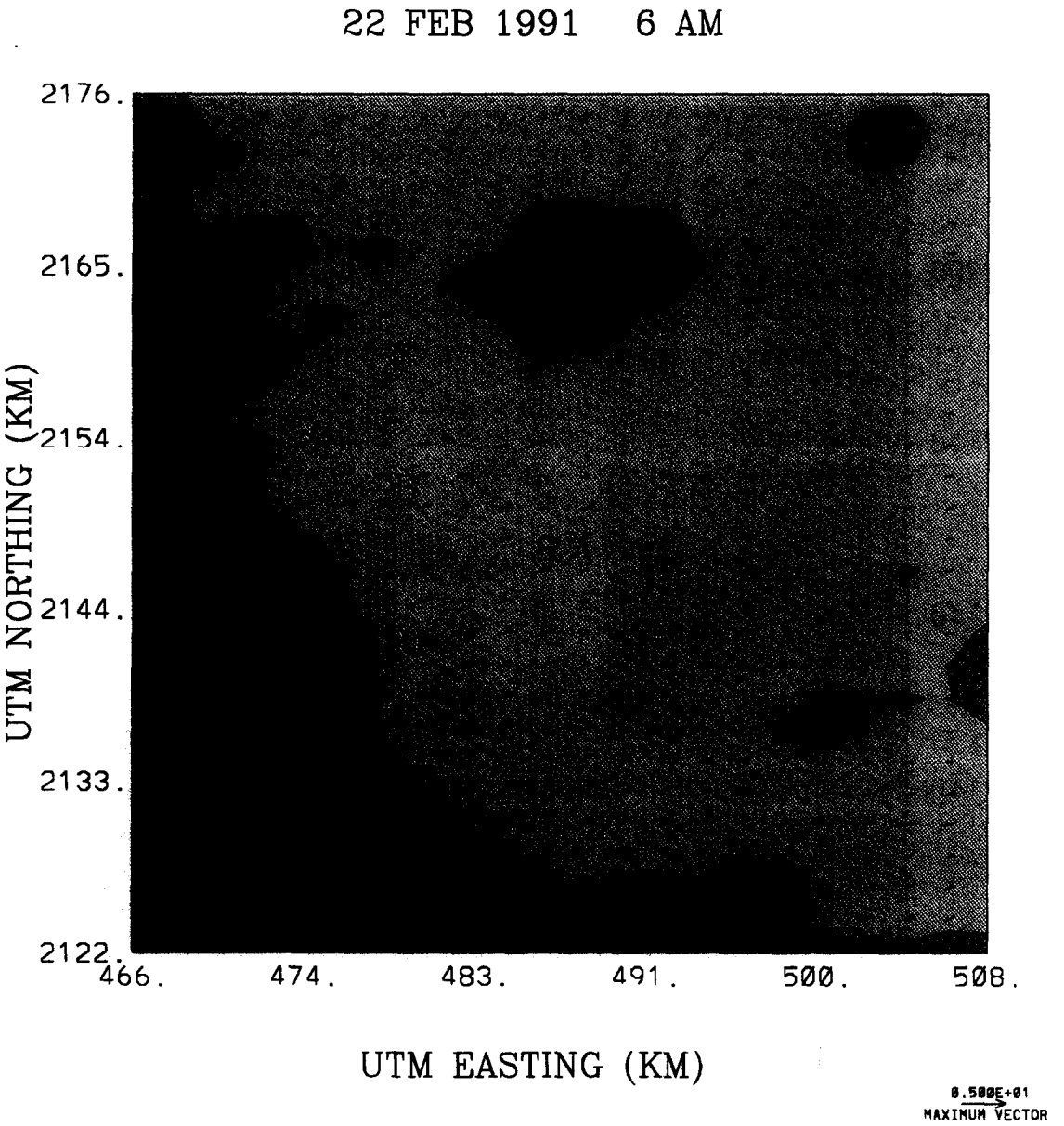

Fig. 2. Comparison of measured winds (red) to computed winds (blue) for 6 a.m., 22 February 1991, with station locations and topography. The beige color represents an elevation range of 2200–2350 m msl, while the dark green region represents an elevation range from 3550 to 3700 m msl.

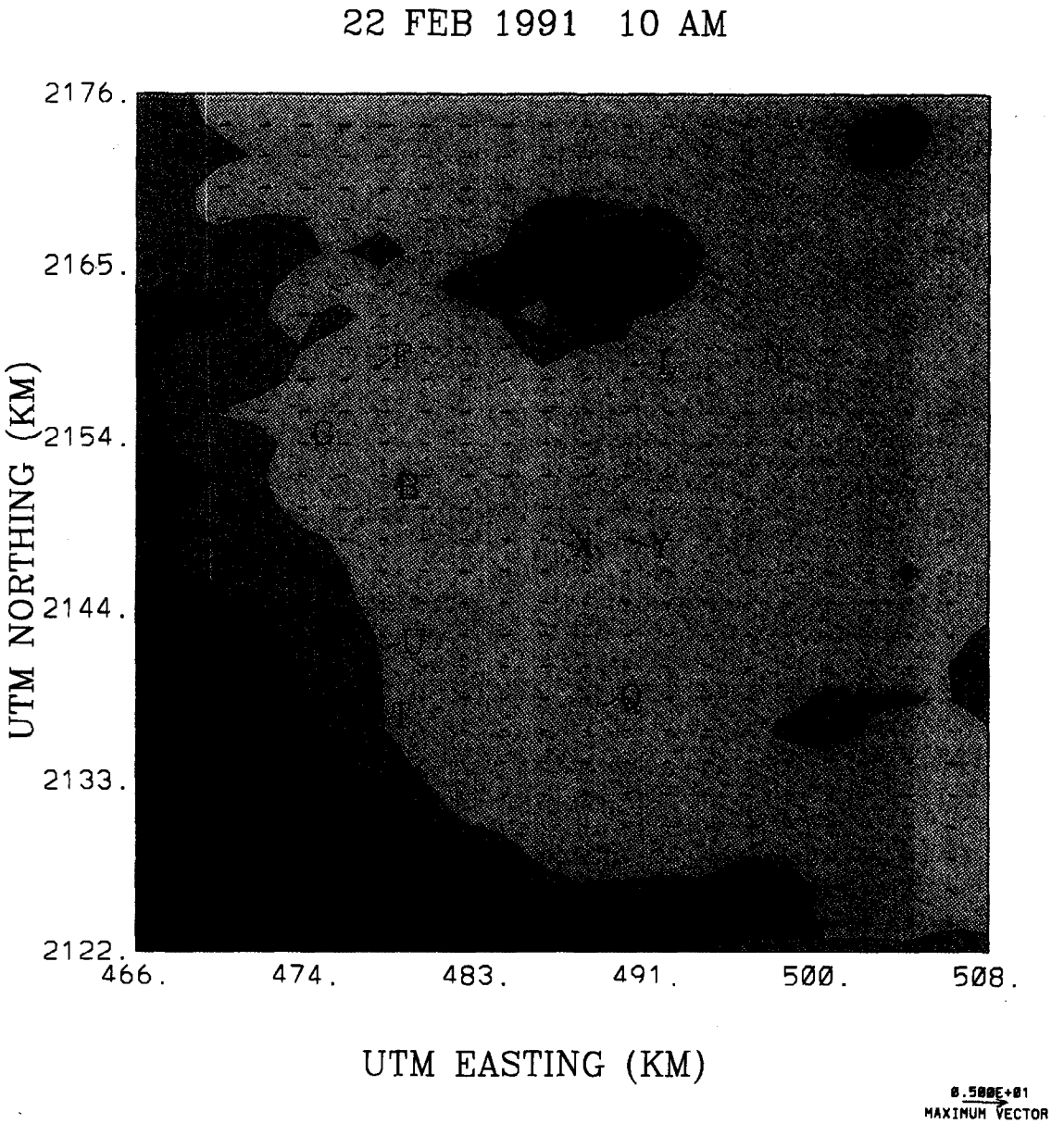

Fig. 3. Comparison of measured winds (red) to computed winds (blue) for 10 a.m., 22 February 1991, with station locations and topography.

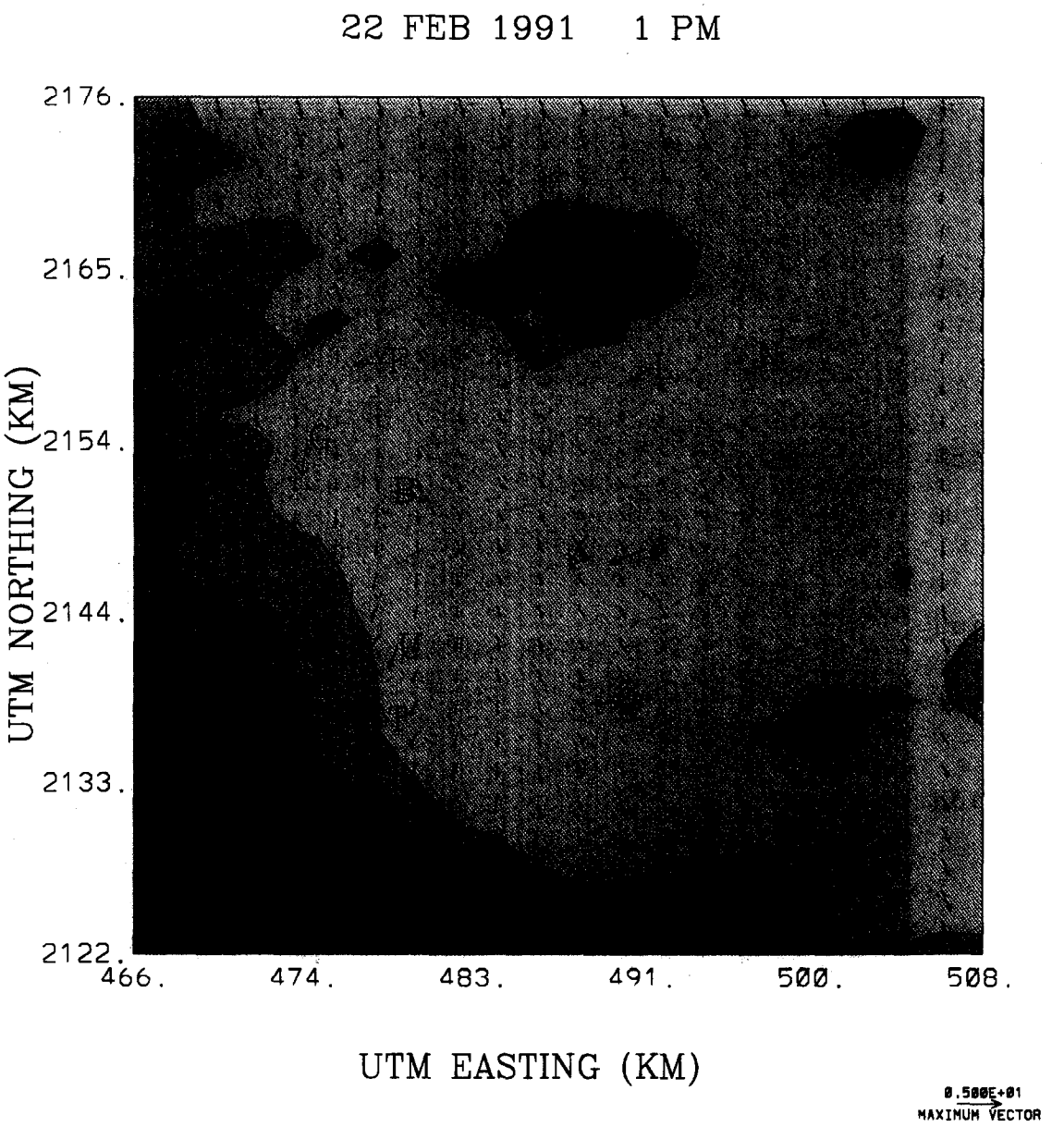

Fig. 4. Comparison of measured winds (red) to computed winds (blue) for 1 p.m., 22 February 1991, with station locations and topography.

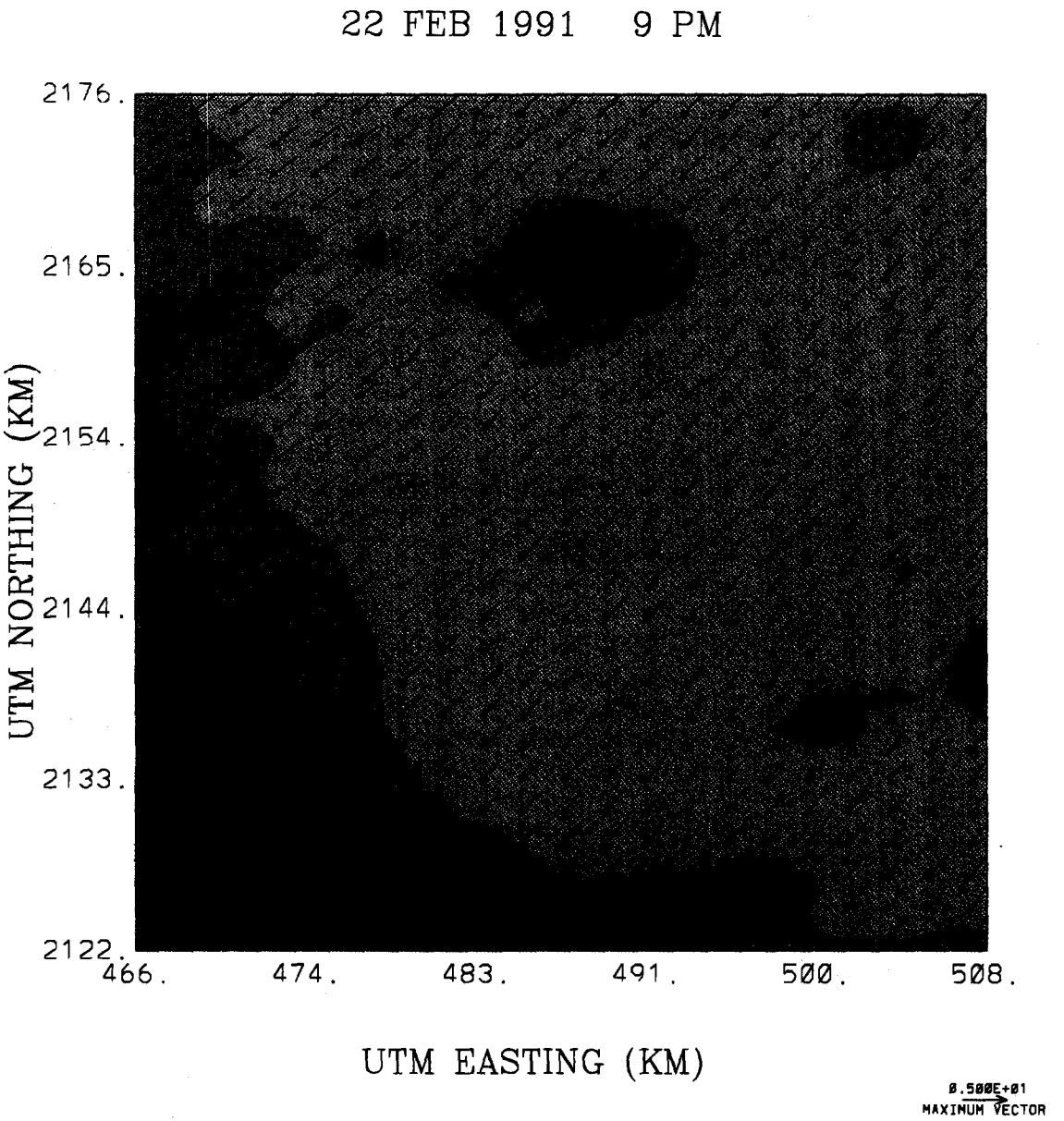

Fig. 5. Comparison of measured winds (red) to computed winds (blue) for 9 p.m., 22 February 1991, with station locations and topography.

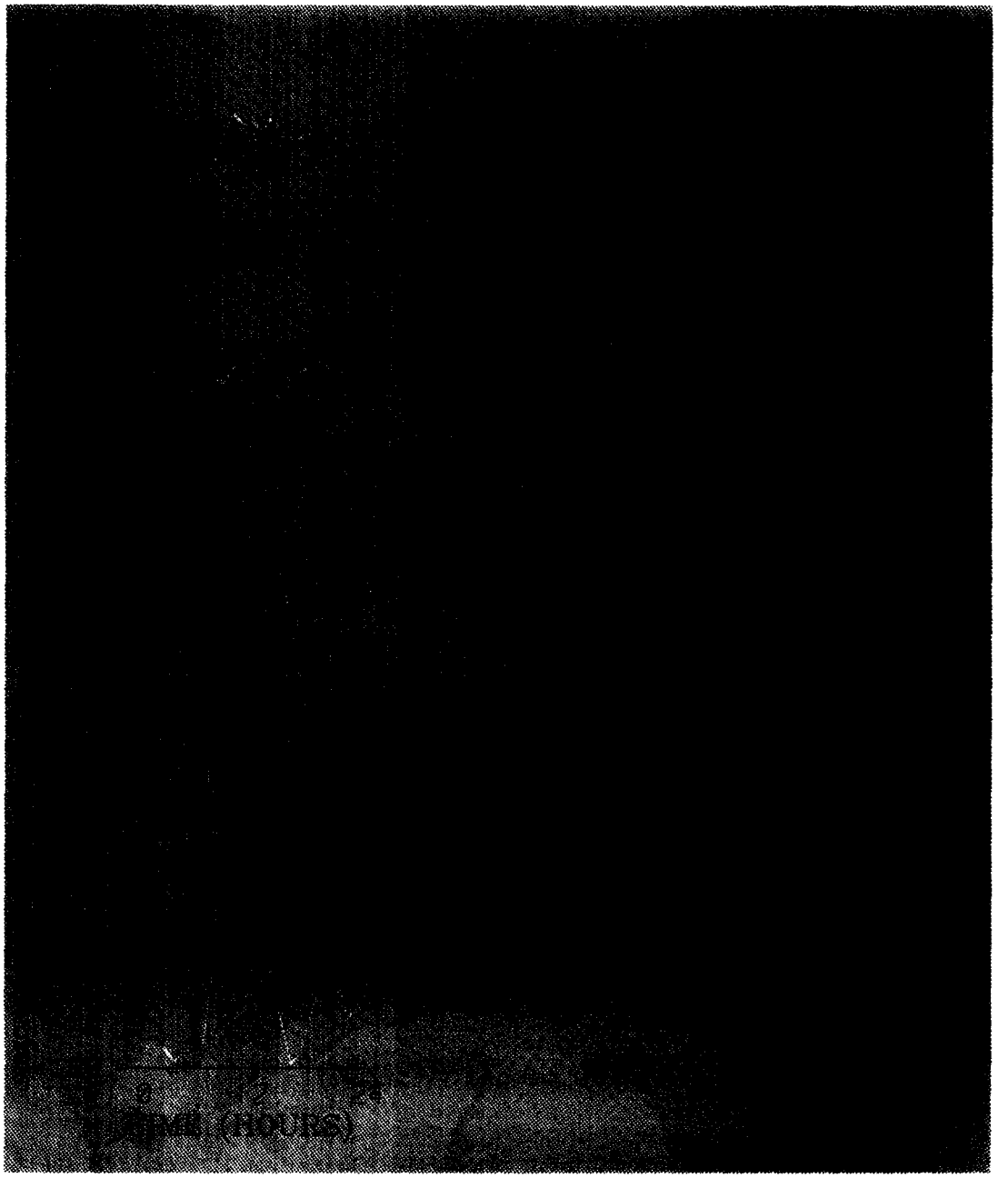

Fig. 6. Comparison of measured hourly wind directions (yellow) to computed hourly wind directions (blue) on 22 February 1991, with station locations and topography.

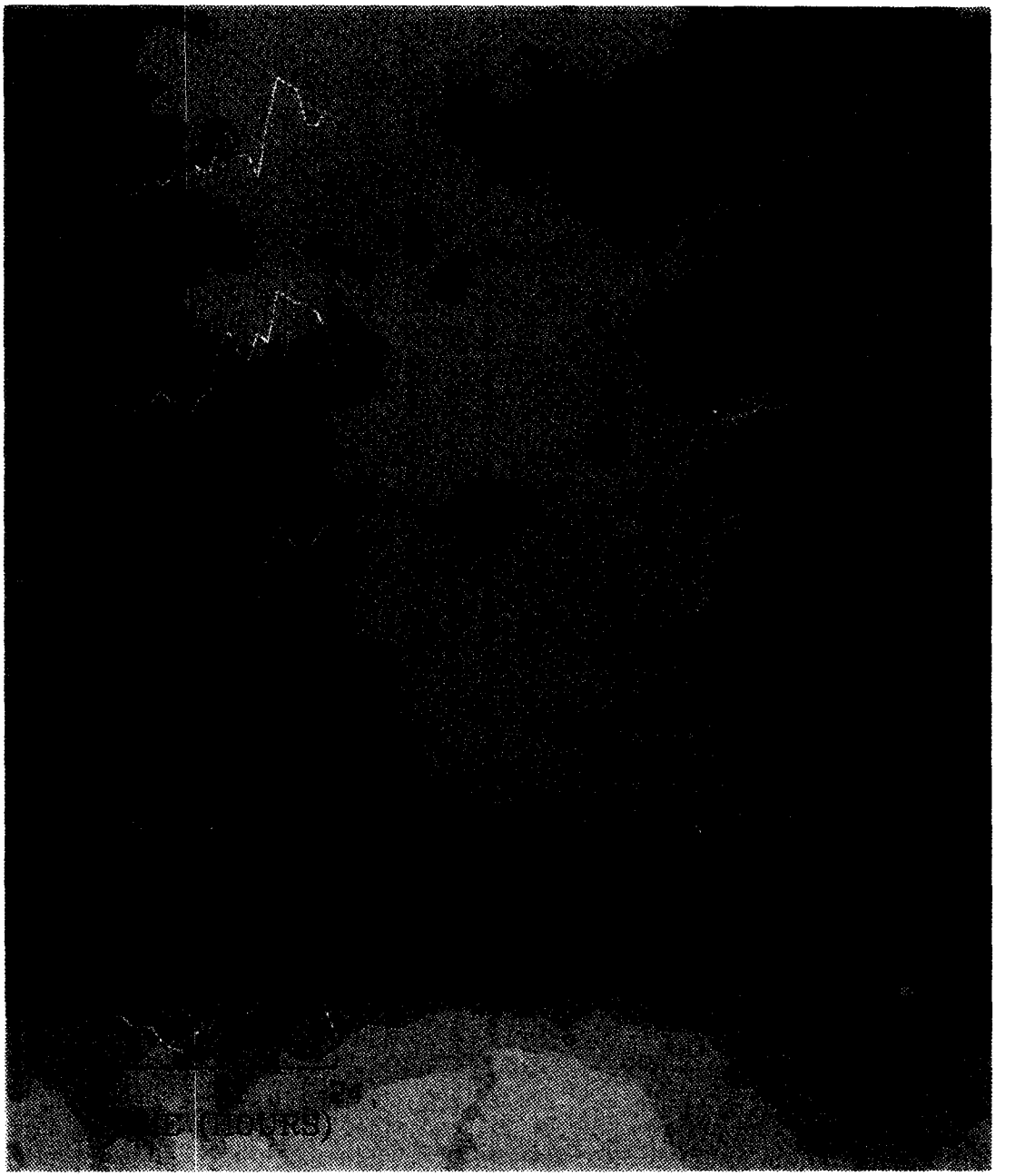

Fig. 7. Comparison of measured hourly wind speeds (yellow) to computed hourly wind speeds (blue) on 22 February 1991, with station locations and topography.

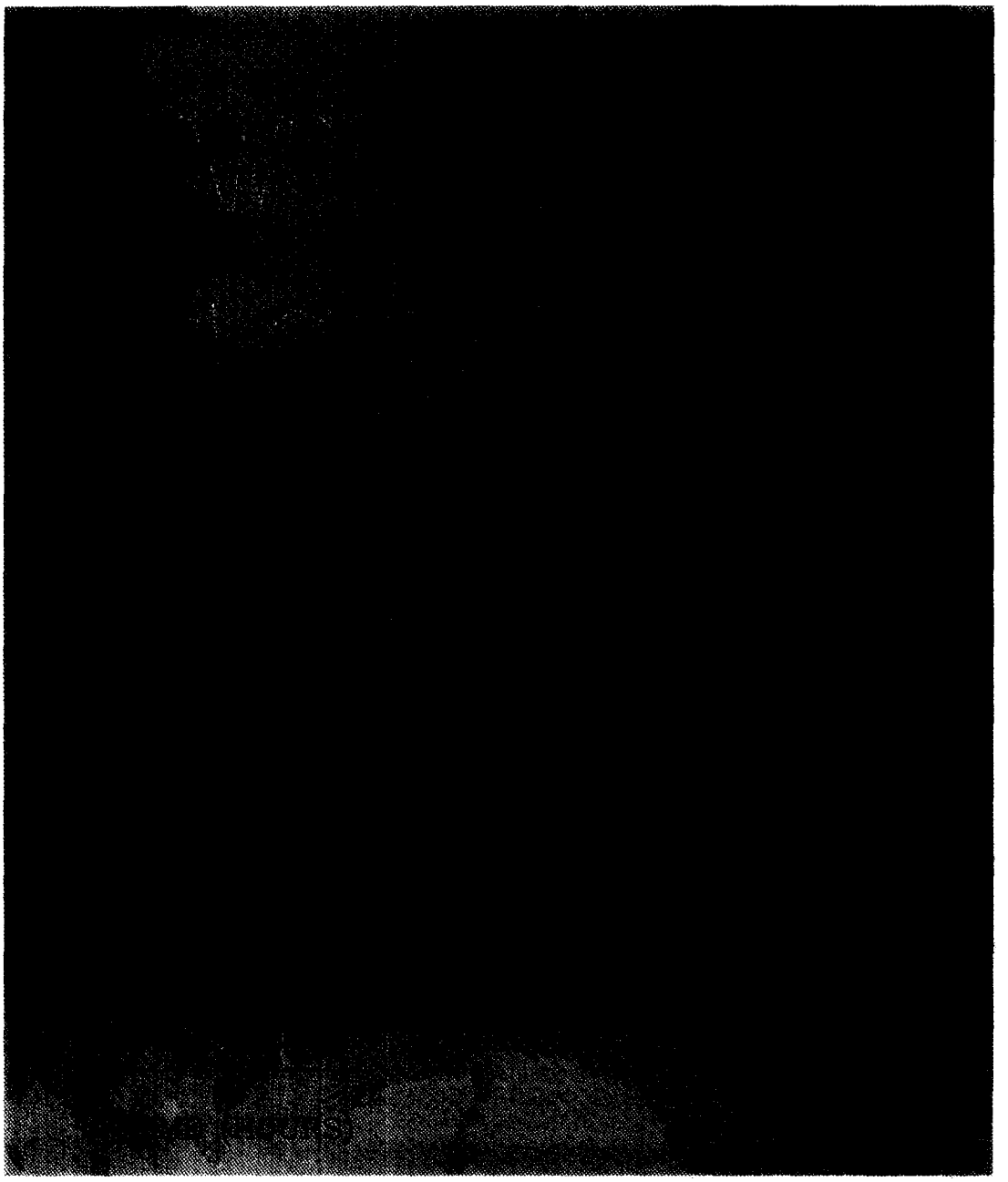

Fig. 8. Comparison of measured hourly wind directions (yellow) to computed hourly wind directions (blue) on 28 February 1991, with station locations and topography.

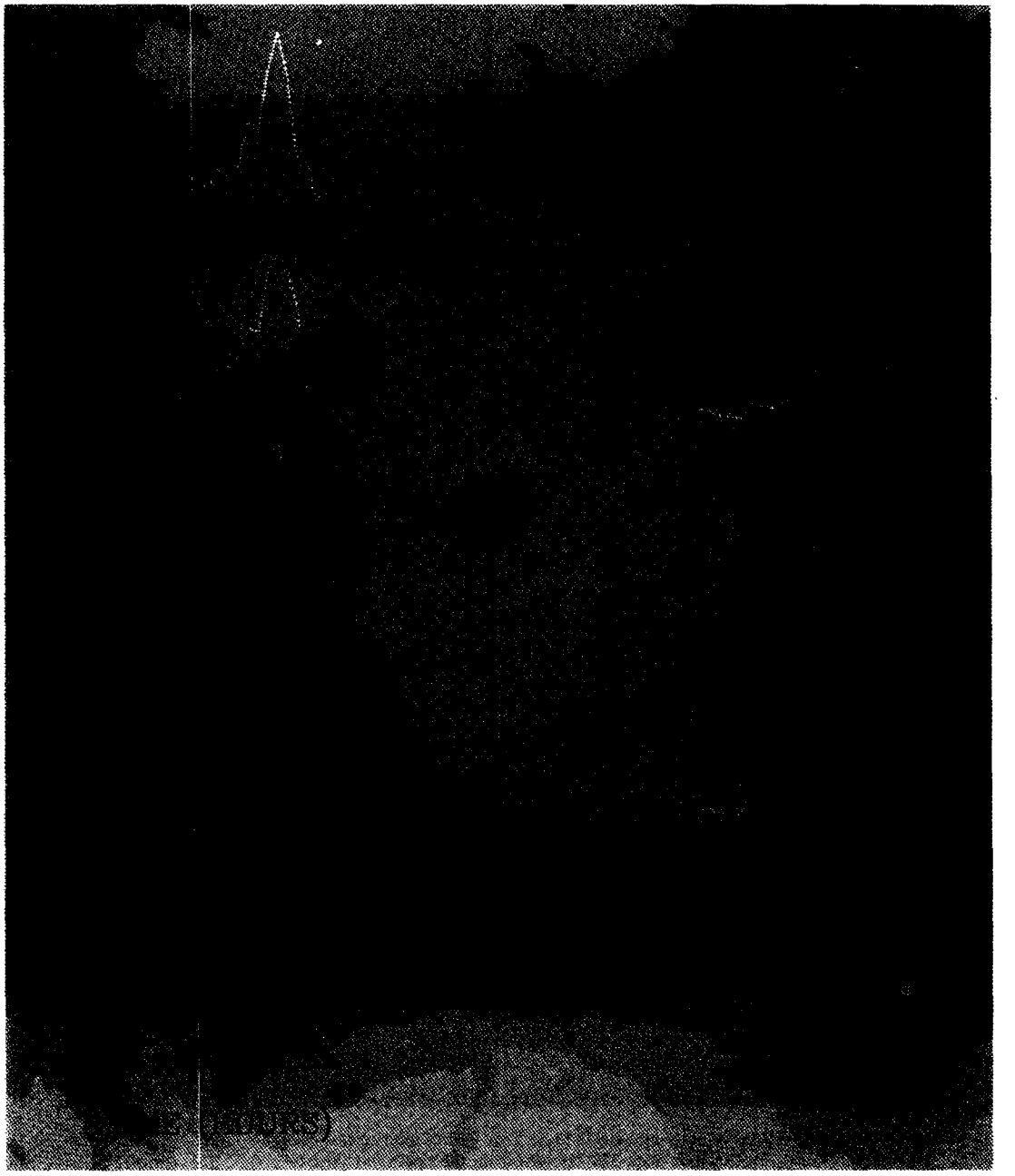

Fig. 9. Comparison of measured hourly wind speeds (yellow) to computed hourly wind speeds (blue) on 28 February 1991, with station locations and topography.

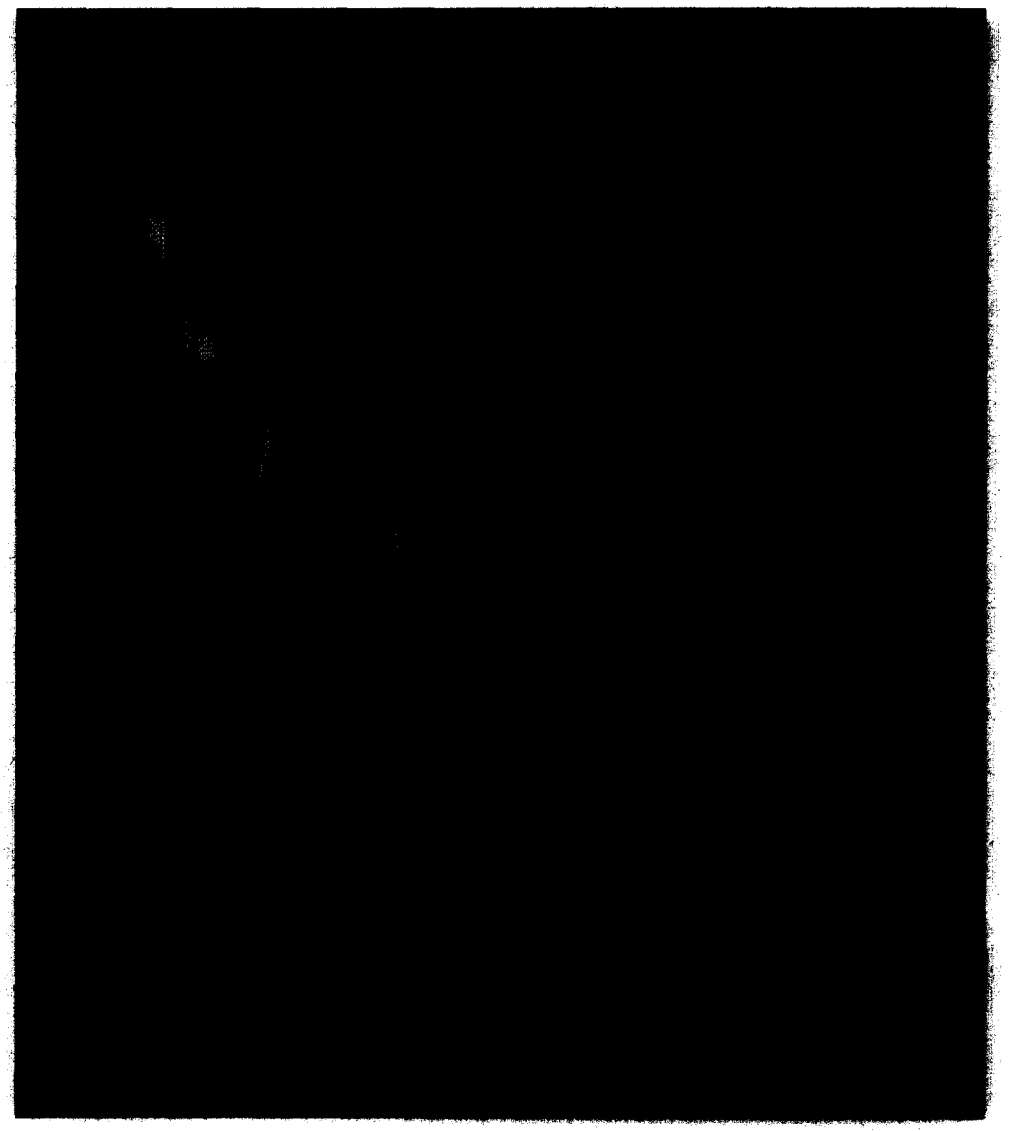

Fig. 18. Pseudo-particles interacting with Pico de Tres Padres after release from a source near Tula with winds from 350° as seen from the north–northeast.

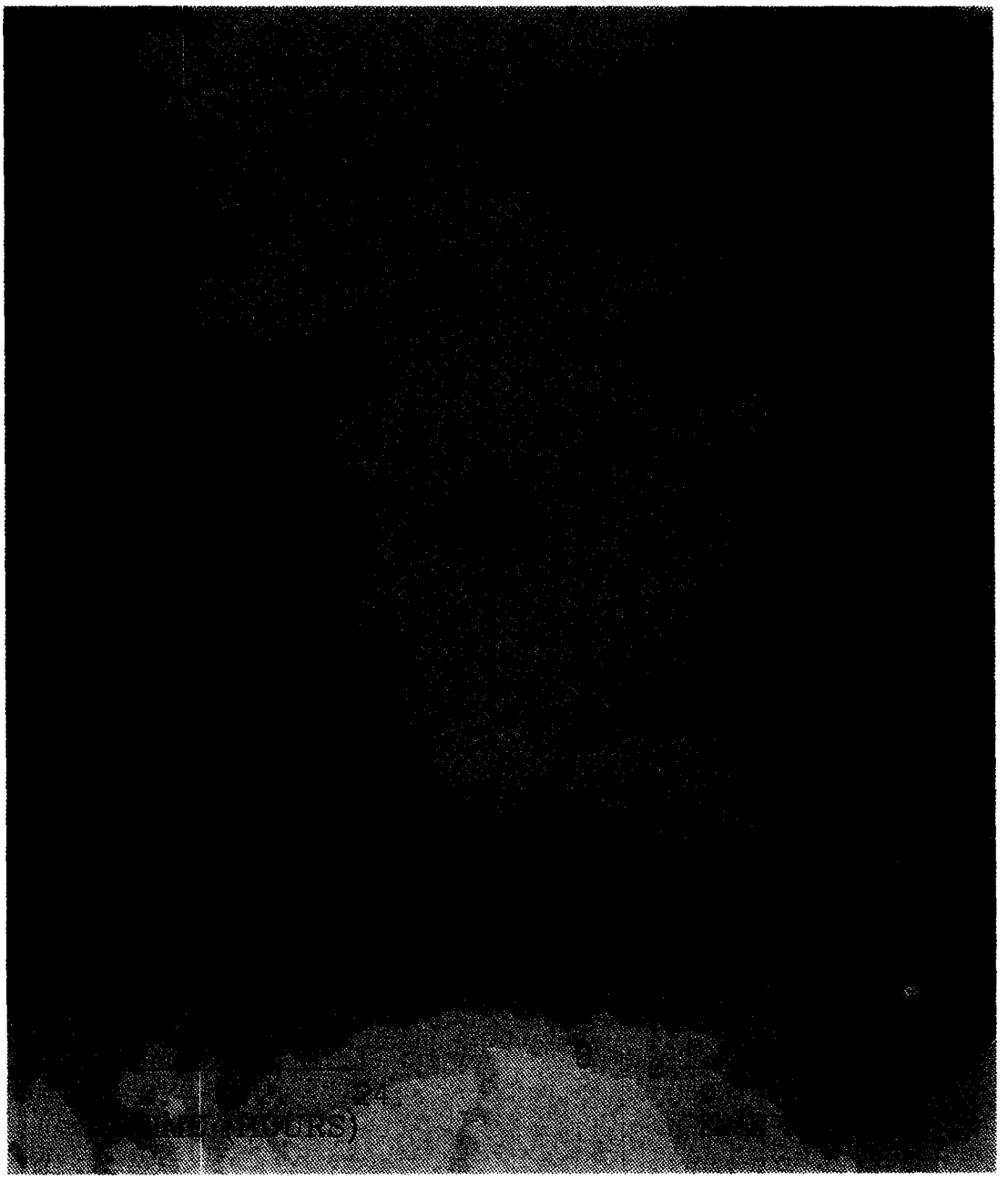

Fig. 25. Comparison of hourly measured CO concentrations (red) from the SEDESOL surface monitoring network with modeled ones (blue) with station locations for 22 February 1991.

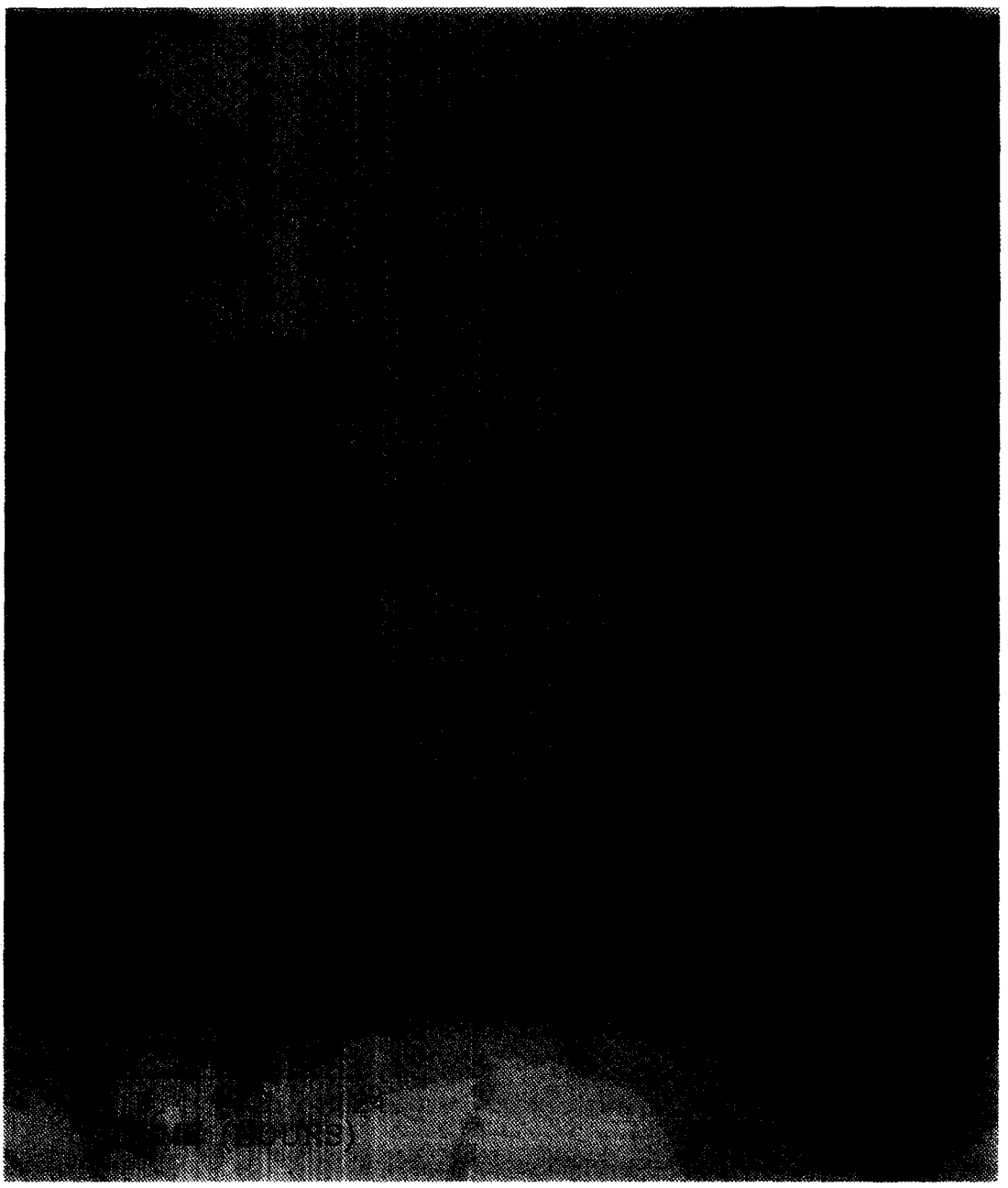

Fig. 26. Comparison of hourly measured CO concentrations (red) from the SEDESOL surface monitoring network with modeled ones (blue) with station locations for 28 February 1991.

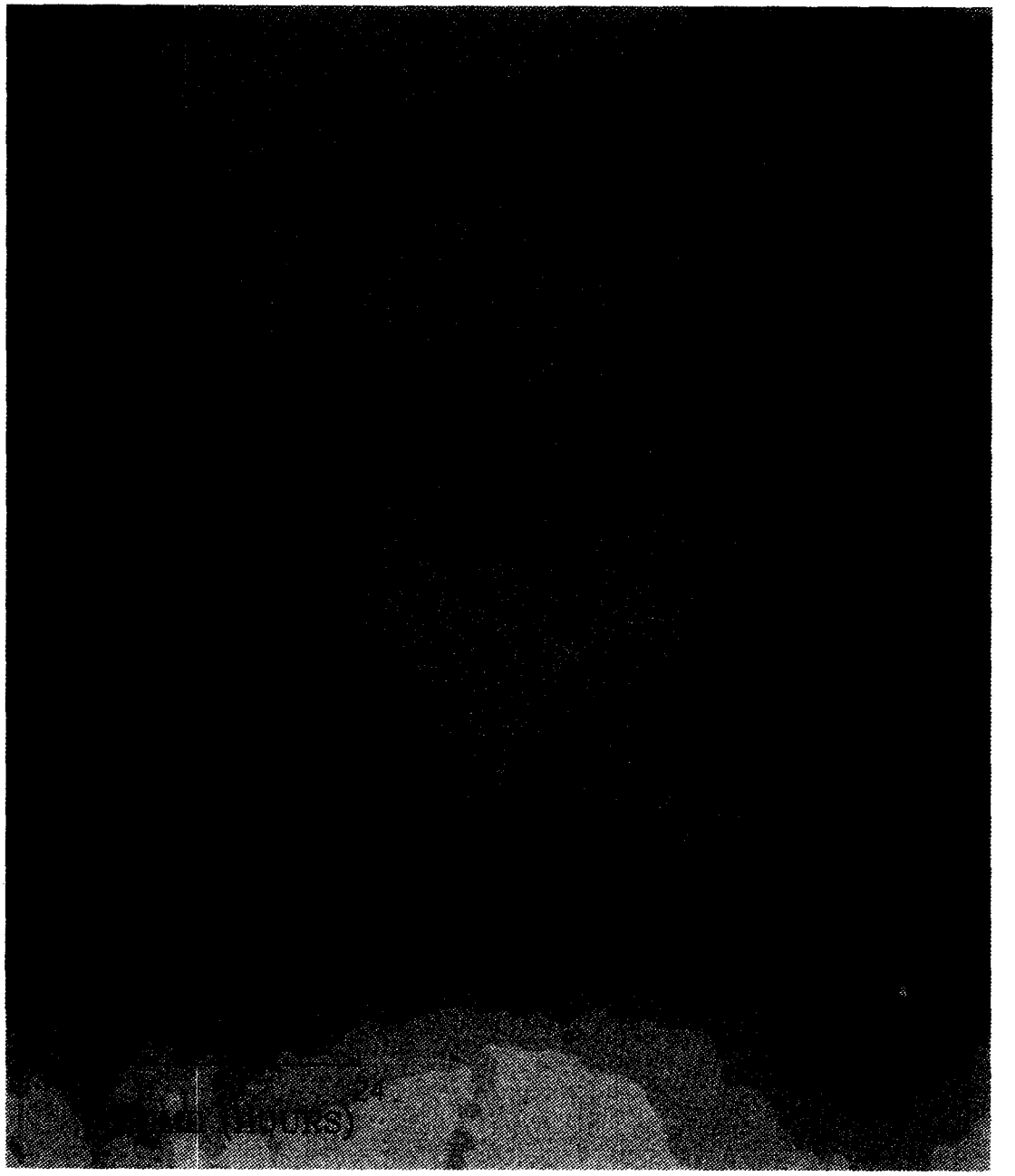

Fig. 27. Comparison of hourly measured SO_2 concentrations (red) from the SEDESOL surface monitoring network with modeled ones (blue) with station locations for 22 February 1991.

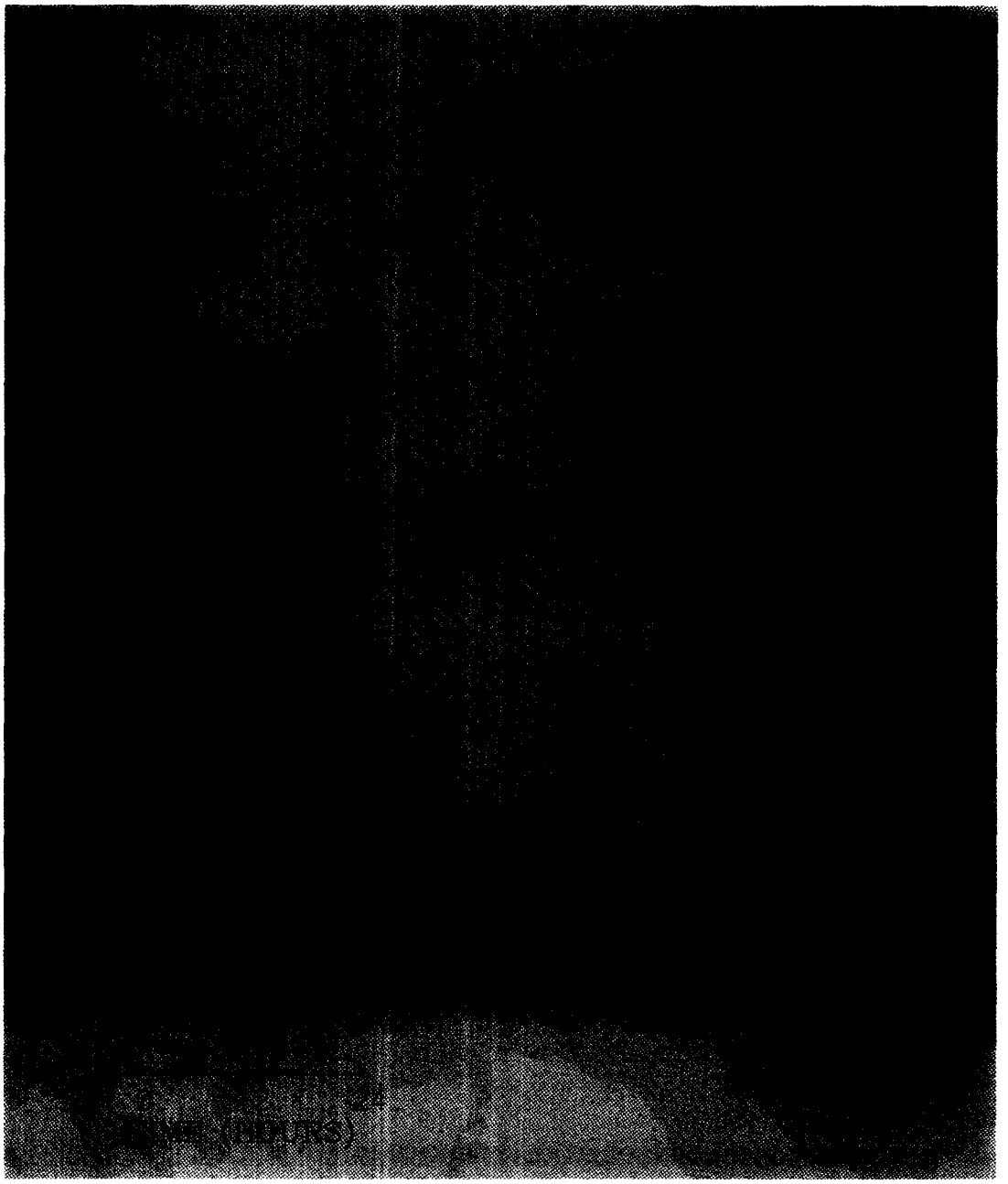

Fig. 28. Comparison of hourly measured SO_2 concentrations (red) from the SEDESOL surface monitoring network with modeled ones (blue) with station locations for 28 February 1991.

pressure systems. In order to have a wind shear in the upper-levels, the model was modified to allow the user to specify the wind at two levels. The result of the coding (prior to this project) was to add additional factors (Yamada and Bunker, 1988) in the conservation equations for the two horizontal components so that the winds were nudged toward the desired winds at the specified levels.

Early in this project, three days representing poor, good, and normal air quality were chosen for detailed modeling. All of the days were in the winter of 1987–1988. Meteorological inputs were based on the afternoon rawinsondes. Although the meteorology of the region could be reasonably represented on days with poor ventilation and consistent upper-level winds, the model gave poor results on days with changing upper-level winds. Hence, we have modified the HOTMAC model to allow for the input winds aloft to vary with time. Hourly nudged winds were computed by interpolating between the two measured winds closest in time. This improved approach, however, still suffered from two deficiencies: (1) the low-level driving winds remain constant unless the user-specified nudging heights were quite low and (2) the differences between the measured winds and the large-scale winds were not considered. The addition of an additional nudging level deals with the first deficiency. In the second case, the measured wind normally reflects both the large-scale wind and the local influences of topography and surface features. The procedure we have developed to obtain an approximate large-scale wind is based on using the model to estimate the local wind in the lowest 500 m. Essentially two model runs are made. In the first run, typical upper-level conditions are used and the low-level nudge winds are kept very small to represent no large-scale forcing. Typically this model run is for one and a half days with one-half day to spin the model up and one day to provide hourly local wind estimates. The modeled local winds are then subtracted from the measured winds to obtain the large-scale component of the wind. This procedure permits the model to reproduce the observations at the measurement site and make good estimates for the rest of the model domain. It also results in good performance over many days without reinitializing the model.

As mentioned earlier, the original version of the model used only two kinds of surfaces: water and land. The urban canopy was approximated by using the estimated distribution of CO emissions defined on a 1 km grid. The relative CO emissions were used to proportion the fraction of the area of a grid cell that was covered by canopy (roof tops) and to estimate the average soil conductivity, average soil heat capacity, and the urban heat release intensity. We changed the model to accept the results of a thirteen category, satellite-derived surface characterization. For each classification, an estimate was made of the associated surface characteristics: (1) surface albedo, (2) surface thermal emissivity, (3) surface daytime Bowen ratio, (4) soil heat capacity, (5) soil density, and (6) soil thermal diffusivity. The land coverage percentages were used with the category values to estimate the appropriate surface characteristics for each grid cell. In the case of the Bowen ratio, simple area-weighted means, as used for the other parameters, were not appropriate. The mean daytime Bowen ratio for a cell was calculated as:

$$b_{\text{avg}} = \frac{\sum_{i=1}^{13} f_i/1 + (1/b_i)}{\sum_{i=1}^{13} f_i(1/b_i)/1 + (1/b_i)}$$

where b_i is the Bowen ratio for the class while f_i is the fraction of the cell covered by the class. This formulation averages the reciprocals of the Bowen ratio. If we considered only two cells, one very wet and one very dry, the average Bowen ratio should be moderate, while averaging the Bowen ratio would give dry conditions and averaging the reciprocal gives moderate conditions.

The buildings, pavement, and heat released by man's activities influence the meteorology in urban areas. There are two basic approaches to deal with this effect. One is to use a different roughness length, while the other is to use a canopy. HOTMAC has a canopy that was developed for forested areas. In the canopy approach, alterations are made to the conservation equations for momentum and turbulence to account for the drag effects (Yamada, 1982). The energy balances are also modified and involve interception of short and longwave radiation by the canopy with associated heating or cooling of the air at the height of the canopy and related changes at the surface (Yamada, 1982). The original canopy was modified to include the anthropogenic energy released by motor vehicles in the lowest few meters of the atmosphere. The current canopy model does not have any energy storage, so that the storage or release of sensible heat occurs only at the canopy bottom (paved streets) and not on the sides and roofs of buildings.

The original version of the model used a very simple treatment of moisture that did not allow for the effects of dew formation and other surface moisture features. A new treatment has been developed in which moisture can accumulate at night on the surface if the temperature reaches the dew point. The next day, the Sun's heating evaporates the surface moisture before heating the surface or the adjacent air. If the surface is dry and the Sun is well up, the Bowen ratio is assumed to be constant. In other words, the energy flux to the atmosphere is apportioned between the heating of the air and evaporation/transpiration of water by a fixed ratio. During the night or when the Sun is low, the evaporation is nil.

3. METEOROLOGICAL MODEL-MEASUREMENT COMPARISONS

Measurements are very important to provide model inputs and to help understand the limitations and performance of the models. For the meteorologi-

cal model there were six types of measurements that were available to provide insight into the model's performance: (1) surface station winds, (2) rawinsonde profiles, (3) Tethersonde profiles, (4) aircraft meteorological profiles, (5) aircraft elevated winds, and (6) lidar-derived mixing heights. It is important to realize that the model and the measurements do not necessarily represent the same parameter. For example, the surface winds are measured at a single site at a height of 10 m (which may be measured from the top of a building) and represent one hour scalar averages of the wind direction and wind speed. On the other hand, the model provides one hour ensemble mean vector averages of the wind over a 2 km by 2 km grid with a vertical depth appropriate to the grid cell. The model takes the ground level as the street level and includes the buildings as the above-ground canopy. The measurement sites are usually chosen to be in more open areas, but they may be influenced by nearby buildings or trees.

Detailed comparisons were made with a variety of measurements during two time periods: 21–22 February and 25–28 February 1991. In the first period there were relatively frequent measurements and high ozone concentrations occurred in the southwest portion of the city on 22 February. This period represents a typical pollution episode. There were fewer measurements available during the second period and the highest ozone concentrations occurred in the western region on 28 February. The second period was chosen to represent a less common pattern that also produced high concentrations.

For both periods, the simulations were begun with information from the late afternoon and early evening rawinsonde measurements at the airport. The balloons are designed to rise at a rate of about 200 m min^{-1}. In the Mexico City work, the data were available at increments of about 75 m in height. About seven rawinsonde flights were made each day. During both simulation periods, the upper-level winds used as model input at 2000 and 3000 m above the surface were based on the rawinsonde measurements.

During the first period, the low-level winds were obtained from a Tethersonde in the northcentral part of the city by averaging the winds between 250 and 750 m. The Tethersonde spends a short time at each height and it takes most of an hour to cover the atmosphere up to the maximum height. In contrast, the rawinsonde takes a much shorter time to traverse the same height and produces data at much larger intervals in height. The model requires an ensemble mean wind and thus the Tethersonde provides a better approximation of the required input. For the second period, when relatively few Tethersonde profiles were available, the rawinsonde profiles were used.

3.1. *Comparison to surface station winds*

Before we begin model-data comparisons, a word of warning must be given. The model produces volume-averaged, ensemble-mean vector winds. These winds are taken from the grid cells nearest to the monitoring locations. The measurements, which were provided by SEDESOL, represent local, scalar-averaged wind speeds and directions. We use the term scalar-averaging to describe the averaging of the wind directions independent of wind speeds and the averaging of speeds independent of directions. In the scalar averaging of the directions the representation of the current wind direction depends upon the value of the previous wind direction and the range of wind directions is taken as 0°–540° to prevent misleading averages. For example, if the wind were from 350° one moment and 5° the next, 365° would be used instead of 5° for averaging purposes. In this example, if the range were limited to 360°, a 5° wind would have been averaged with a 350° wind to provide an average of 172°. In addition to the averaging techniques, stations may have local influences which could not be resolved by the model.

There are two kinds of displays which were developed to help understand the model performance: (1) hourly surface plots in which the model wind vectors are shown along with the measured winds and station locations, and (2) daily time-profile plots in which either the wind direction or the wind speed is compared to the measurements. In both cases the terrain is also shown as well as the locations of the measurement sites. Figures 2–5 show hourly simulations of the vector fields on the inner grid for the morning, morning transition, afternoon and evening, respectively, for 22 February. The dark green in the lower left-hand corner of the figures represents the mountains to the southwest of the city. The symbol Y represents the Hangares station of the SEDESOL network, which is located at the airport. The mountains in the upper central area are Pico de Tres Padres which are north of the city center. The blue arrows show the modeled wind speed and direction (not shown if the winds exceed 5 m s^{-1}), while the red arrows show the measured wind speed and direction (no arrow is shown if the data are missing or the speed is zero). The modeled values are at a height of 26 m in the terrain following a coordinate system which corresponds to about 40 m above the ground. This height was chosen because it is the first height above the highest point of the canopy for which calculations were made.

The 6 a.m. slope winds are well represented as evidenced by stations U and T which are closest to the mountains (Fig. 2). Station B is not well represented, but it generally seems to show anomalous behavior (see Figs 2–5). The measured winds at city stations such as X and Y show a somewhat different behavior than the modeled winds which might be produced by local effects of buildings. The measurements also suggest that there is more wind convergence over the city than the model shows, as seen by predominately westerly winds on the west side of the city and the predominately easterly winds on the east side of the city. The transition to upslope flows occurred at about 10 a.m. when the model showed a less developed

transition than the measurements (Fig. 3). At 1 p.m. Fig. 4 shows the afternoon flows with fully developed slope winds. At 9 p.m. strong winds out of the northwest dominate the flow fields and there is good agreement between the model and the measurements (Fig. 5). This wind is probably the result of a slope wind that originates near the Gulf of Mexico. Model simulations with Regional Air Modeling System (RAMS) model and a large enough domain to include both oceans predict the occurrence of these winds. These four figures demonstrate the variety of wind conditions which can occur in the valley during a single day. They also show that the model does a reasonably good job of representing the major features.

Time profiles of wind directions and wind speeds at all sites on 22 February are shown in Figs 6 and 7, respectively. In Fig. 6, the entire model domain is shown: the two white points on the lower right-hand side are the two 5300 m plus volcanoes, the central green splotch is Pico de Tres Padres, while the red Y is the airport. The model shows good behavior for stations U and T, although there are some large fluctuations in the measurements which may be the result of afternoon clouds which are not represented in the model.

The wind speeds shown in Fig. 7 represent a fair agreement in the early morning hours and the late evening hours, but they underestimate the increase in the late morning and afternoon winds. Part of this difference may be related to the difference between vector-averaged winds and scalar-averaged speeds. Actual experiments reported by Dr Hector G. Riveros R. of the Instituto de Física at UNAM show that the scalar averages can be as much as 100% greater than the vector averages during circumstances where the mean winds are light and the turbulent fluctuations are large. In more typical circumstances the scalar winds are within 25% of the vector winds. There were light winds and high turbulence levels from mid-morning through mid-afternoon. In the early evening when some of the largest discrepancies are found, the winds were much higher and little difference would be expected between vector and scalar averages. We also performed some experiments in which we tried to model the difference between scalar and vector averages and found that the difference between vector and scalar averages was unlikely to account for the bulk of the model-measurement differences. From an air pollution standpoint, the vector average is more relevant to answer the critical question of how long the same air mass remains near the source and absorbs fresh emissions. The large discrepancy between the modeled and measured wind speeds may be associated with the slope wind from near the Gulf of Mexico which arrives in the late afternoon. Since the effect is not developed dynamically in the model due to the limited domain size, the slope winds are artificially introduced into the model through nudging. The model simulation, therefore, does not allow for either the enhanced stability associated with the slope wind phenomenon or the resultant, large, wind shear between the top of the slope-wind layer and the southwesterly winds aloft. The weaker stratification in the model simulation allows for more mixing between the southwesterlies and the slope wind which results in lower wind speeds at the surface. An additional problem is related to the model's longwave radiation which is discussed in Section 3.2.

Figure 8 shows the comparisons between measured and modeled wind direction profiles for 28 February, while Fig. 9 shows the comparisons for wind speeds. The simulations show relatively good agreement despite the fact that the winds were driven with rawinsondes and the fact that the simulation extends for a relatively long period. The wind speed comparisons show a similar behavior to that found on 22 February.

3.2. *Rawinsonde profiles*

One concern in the comparison of model winds to the rawinsonde winds is the relatively short time over which the rawinsonde measurements are made. The difficulty of a brief measurement period is that it may not be very representative of the average conditions which the model is asked to predict. This concern is particularly important during the daytime, when the wind fluctuations are large. Since the effective averaging time of the rawinsonde measurements is very much smaller than the timescale of the convective eddies, one can approximate the variance in the measured mean by using the model-computed velocity fluctuations σ_u and σ_v. Figure 10 is an example of such a comparison for 22 February 1991. The solid line shows the measured wind directions and wind speeds by the rawinsonde, the dotted line shows the model predictions, while the asterisks show twenty randomly selected model realizations. In the lower 50 m agl only two model heights were shown to improve readability. Very close to the surface, the asterisks indicate that most of the winds are consistent with the model, because the turbulent fluctuations are so large. The modeled winds in the afternoon are generally representative of the measurements although the large spread in the asterisks suggest that the measurements are unlikely to be very precise representations of the mean winds. There are some large discrepancies between the measurements and the model results in the morning with 5 a.m. the most striking example. At 5 a.m. the large wind shear suggests that using more points from the measured profile in the nudged wind profile would improve the simulations. Near the surface there is a high speed tail in the afternoon measurements which is likely to be a very local effect or perhaps the balloon has been launched from a point other than the assumed point. The odd feature of a high speed tail is a frequent feature in the rawinsonde measurements.

The very low, modeled turbulence in the 200–750 m layer is apparent in the morning as the asterisks show little spread between the surface and 1 km. High levels

of turbulence remain at the surface and also appear in the layer from 1 to 2 km where the high wind shear is important.

Figure 11 compares the modeled (dotted line) and measured (solid line) potential temperatures and water vapor concentrations during the morning and afternoon hours on 22 February. In the morning hours, both curves show a stable atmosphere near the surface, but the measured atmosphere is considerably more stable. The model appeared to be overestimating the incoming long-wave radiation. Typical modeled long-wave radiation values of about 285 $W m^{-2}$ were obtained while Oke *et al.* (1992) reported average values of 270 $W m^{-2}$ in February of 1985 for Mexico City. The model's long-wave radiation module has since been improved with the result that the potential temperature profiles are close to the measured ones. The afternoon potential temperature and moisture comparisons show a similar behavior in both the model and the measurements. In the morning, the model misses some of the lower-level, water-vapor variation, while in the afternoon the comparison is good. The increased water vapor levels near the surface in both the model and the measurements are associated with evaporation or transpiration at the surface.

Figures 12 and 13 show the results of model and measurement comparisons for rawinsondes taken on the 25th and 26th of February. The model is quite successful in tracking major changes in upper-level winds. It is also clear that the wind fluctuations are quite important.

The problem of representative upper-level data is an important one and the wind simulations suggest the rawinsondes are telling us less than we thought. This problem is important not just for Mexico City air quality, but also for weather forecasting and air quality analyses throughout the world because rawinsondes are relied upon for most meteorological and air quality analyses.

3.3. *Aircraft meteorological profiles*

There were four days, the 21st, 22nd, 26th, and 27th of February 1991, in which vertical profiles were measured by aircraft during the two periods of interest; there were also measurements along an east–west traverse at 500 m above the surface taken on the first three of these days. In each case, the plane took off from the airport in midmorning and climbed out to the northeast. The measured profiles are compared to the profiles calculated by the model for the airport location (station Y). The comparison of wind directions and wind speeds is shown for the first three days in Fig. 14. Generally, the model provides a reasonable representation of the measurements, although it does tend to give lower wind speeds near 1 km where a frequently higher speed wind occurs. There is no direct input of these winds into the model, because the model uses only the rawinsonde or Tethersonde, height-averaged winds below 750 m and the rawinsonde winds at 2000 and 3000 m above the surface for nudging. The effect of these higher elevation winds might explain some of the discrepancy between the modeled and measured surface winds in the afternoon. After mixing reaches above 700 m, the effect of these winds will be felt at the surface. The other feature of note is the marked fluctuations within the mixed layer. The aircraft measurements have a very short averaging time of one second and show the effects of turbulent fluctuations. The modeled values represent ensemble means and thus do not show the fluctuations, although similar values would be expected from the modeled turbulence.

3.4. *Aircraft elevated winds*

There were three mornings, the 21st, 22nd, and 26th of February 1991, in which aircraft measurements of winds were available at about 500 m above the surface during a 25 km west to east flight over the center of the city (approximately 2150 km UTM northerly). Figure 15 shows the comparisons with wind directions and wind speeds for these days. The modeled wind directions were too northerly on two of the days, and the speeds were too light on the other day. In addition, there seems to have been an increasing trend in wind speeds toward the east which was not apparent in the measurements.

3.5. *Lidar mixing heights*

There were four days in which lidar mixing heights were available during the period of interest. The lidar mixing heights were determined as the height at which 50% of the horizontal area has a signal characteristic of the clean air aloft. The calculation of the modeled mixing heights is described in Section 5.2. Two sites were used during the four days. On 22 February, the lidar was at the CINVESTAV site which was a few kilometers north of the city center. On 26–28 February, the lidar was at the UNAM site which was on the southern boundary of the city. The UNAM site was about 100 m above the level of the city and the mixing height measurements are relative to the height of the site. The actual site path was over the city with a lower elevation, taken such that the mixing heights would be expected to be about 100 m higher than those reported. Typically, the lidar cannot identify structures below about 100 m because of line of sight restrictions caused by nearby objects.

Figures 16 and 17 display the comparison of mixing heights between the model and the measurements for 22 February and 26 February, respectively. The agreement for 22 February is excellent. The principal disagreements are in the night when the lidar minimum heights may be important and in the late afternoon when clouds could have influenced the comparison. The agreement for 26 February is also good, however, in the mid-morning the measurements show a much slower increase in the mixing height which was the consequence of the model's underprediction of the early-morning stability.

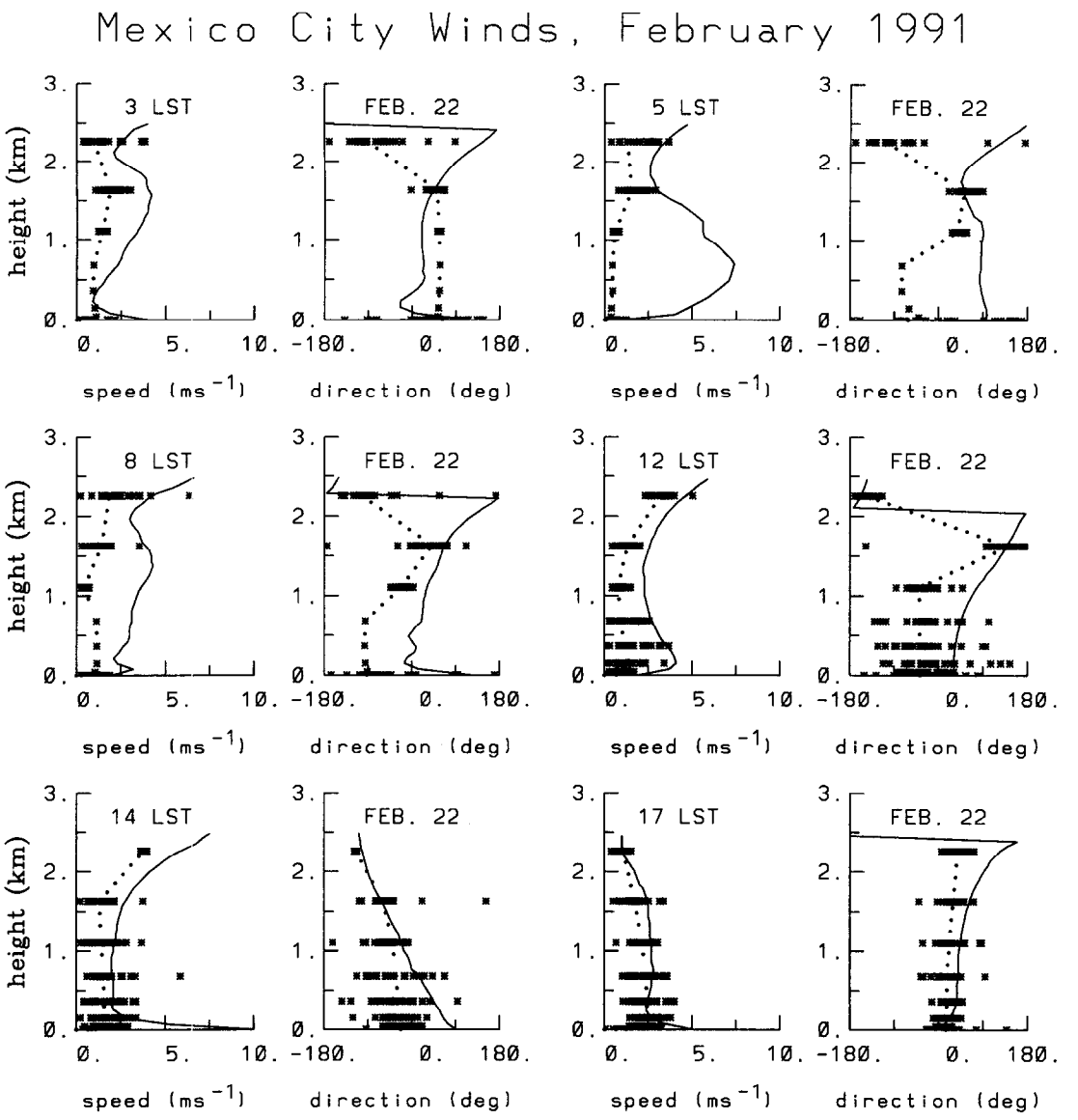

Fig. 10. Comparison of measured wind directions and wind speeds (solid) to modeled mean wind speeds and directions (dotted), and to twenty model realizations (asterisks) for the morning and afternoon hours of 22 February 1991.

4. METEOROLOGICAL MODEL PERFORMANCE SUMMARY

Tesche *et al.* (1990) among others, have suggested a suite of statistical and graphical measures for evaluating the performance of photochemical models. Included among the statistical measures are: model means, observational means, standard deviation of model estimates, standard deviation of observations, least-squares regression statistics, root-mean-square error, systematic root-mean-square error, unsystematic root-mean-square error, index of agreement, skill error and skill variance. The index of agreement is formed by subtracting from 1 the product of number of samples and the squared error divided by the sum over all samples of the squared absolute value of the sample deviation from the sample mean plus the predicted deviation from the sample mean. When the index of agreement is one, the predictions are perfect, while an index of zero means the predictions are noise. The skill error is the ratio of the unsystematic root mean square error to the standard deviation of the observations. The skill variance is the ratio of the standard deviation of the predictions to the standard deviation of the observations.

The computation of these statistical parameters is straightforward for the wind speeds and mixing-layer heights, but wind directions pose a more difficult problem. Because of the difficulty with circular data, techniques developed by Mardia (1972) were used to

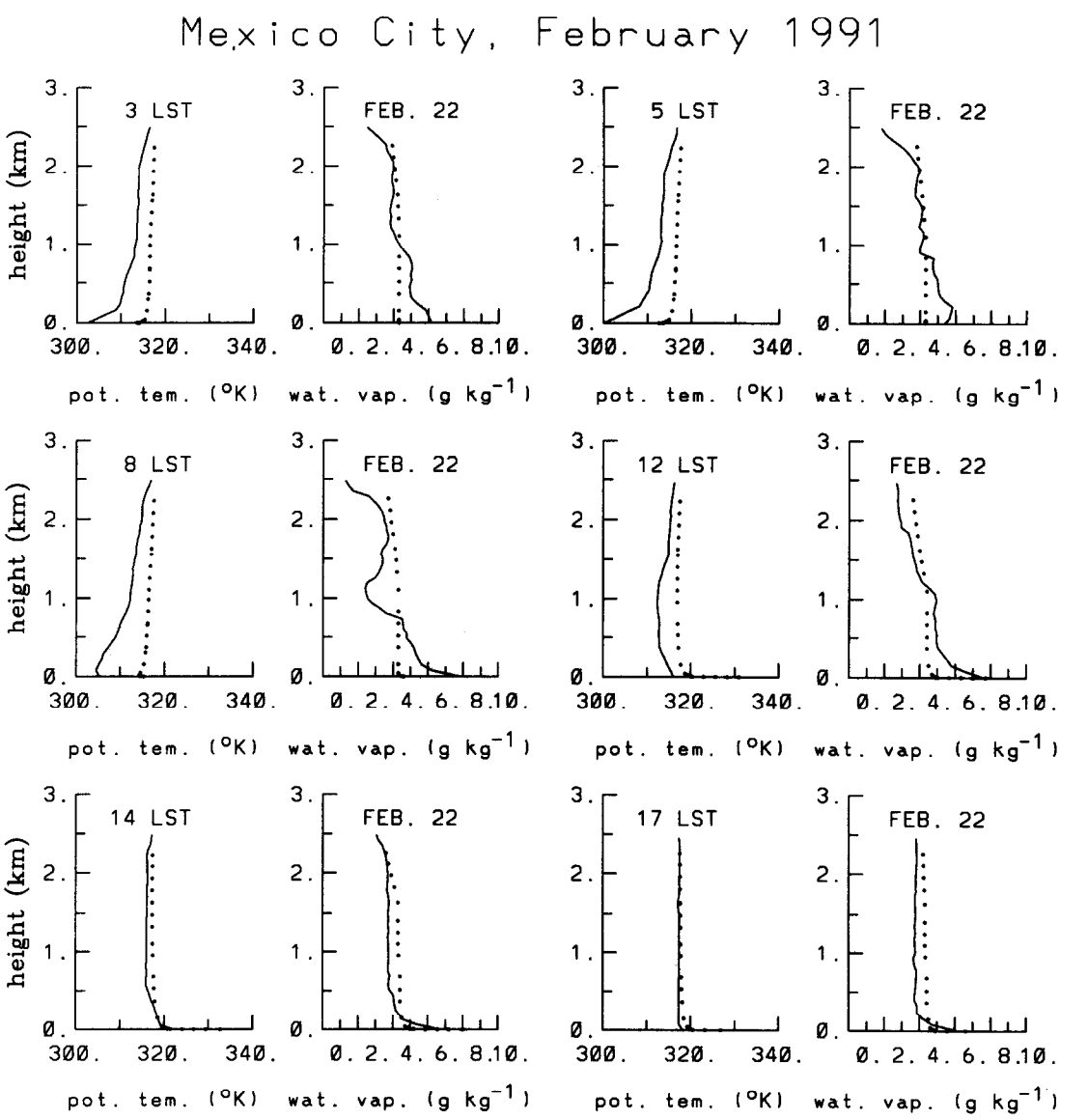

Fig. 11. Comparison of measured potential temperatures and water vapor concentrations (solid) to modeled potential temperatures and water vapor concentrations mean (dotted), for the morning and afternoon hours of 22 February 1991.

calculate a regression relationship which is analogous to the standard regression on a line.

Table 1 summarizes the statistics for wind speeds and directions at the monitoring stations for six days and the lidar mixing height comparisons for four days. Note that the systematic root-mean-square error for wind speed is almost equal to the total root-mean-square error for wind speeds so that most of the error comes from the systematic underprediction of wind speeds. The correlation coefficient for wind directions is not shown, since it is not calculated for circular data.

Generally the model captures the major meteorological features. The winds respond well to major changes in forcing winds and the slope winds develop appropriately and couple well with the large-scale conditions. There are some areas, however, which could be improved. For instance, the model does not have quite as much convergence over the city as it should and it also looks as though the temperatures do not drop as much at night as they should. The different times of the rapid rise in mixing heights in the 25–28 February simulations is of concern and probably related to the temperature behavior. The modeled wind speeds seem to be a little low. The light wind speeds could be a function of the way layer-averaged winds were used as input or they may reflect the fact that the model is currently not using some of the information from the surroundings in the range from 750 to 2000 m above ground. In a layer where

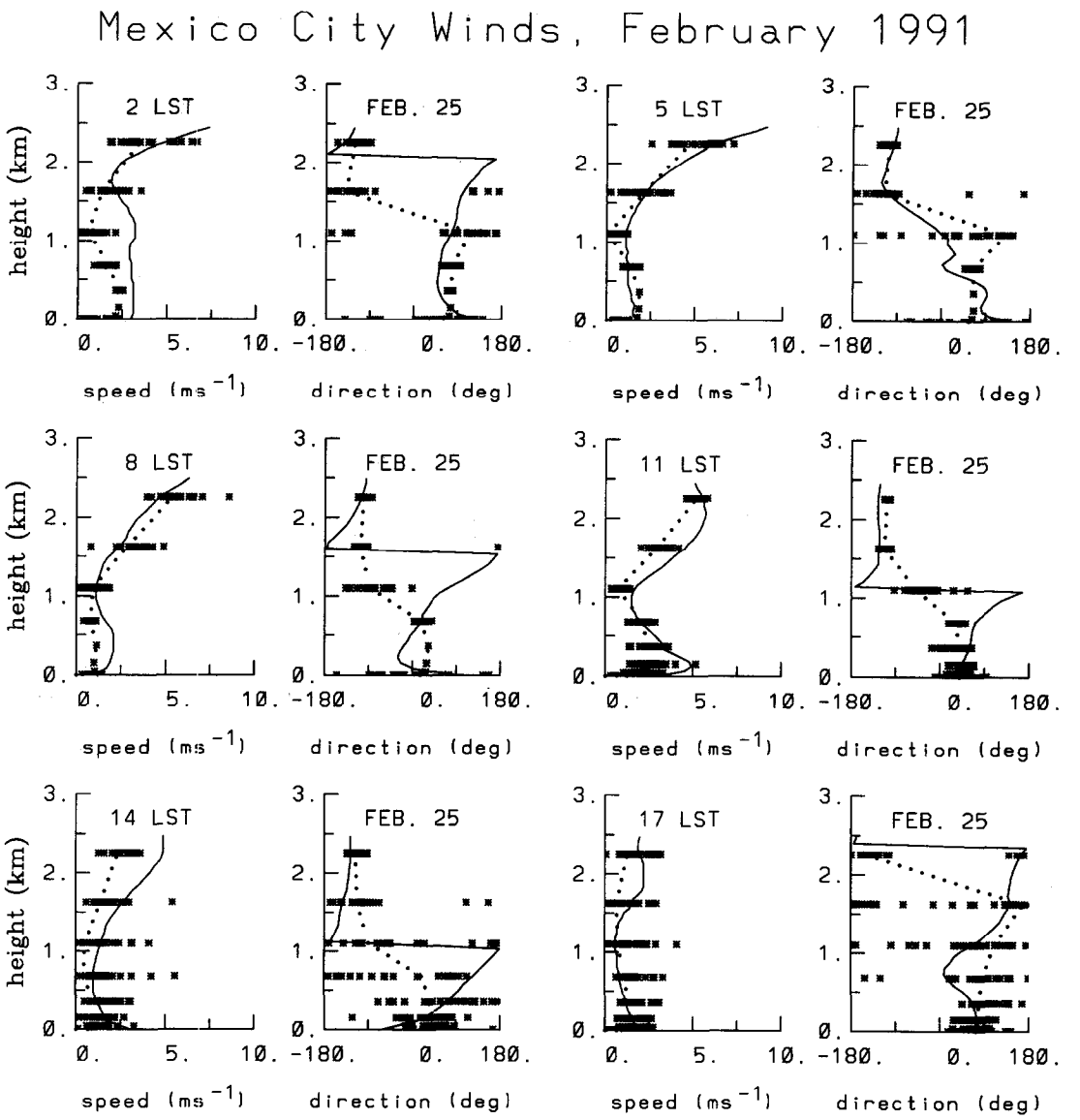

Fig. 12. Comparison of measured wind directions and wind speeds (solid) to modeled mean wind speeds and directions (dotted), and to twenty model realizations (asterisks) for the morning and afternoon hours of 25 February 1991.

Table 1. Statistical comparison of model and measurement surface winds and mixing heights

Parameter	Wind direction	Wind speed	Mixing height
Model mean	161.0	2.4	1274.0
Observation mean	203.0	4.8	1101.0
Standard deviation of predictions	74.0	1.2	1135.0
Standard deviation of observations	94.0	3.0	1043.0
Regression intercept	79.0	1.8	281.0
Regression coefficeint	0.42	0.14	0.90
Correlation coefficient	xx	0.32	0.83
Root-mean-square error	87	3.7	659.0
Systematic root-mean-square error	80.0	3.5	200.0
Unsystematic root-mean-square error	72.0	1.2	628.0
Index of agreement	0.73	0.49	0.90
Skill error	0.96	0.40	0.60
Skill variance	0.79	0.42	1.09

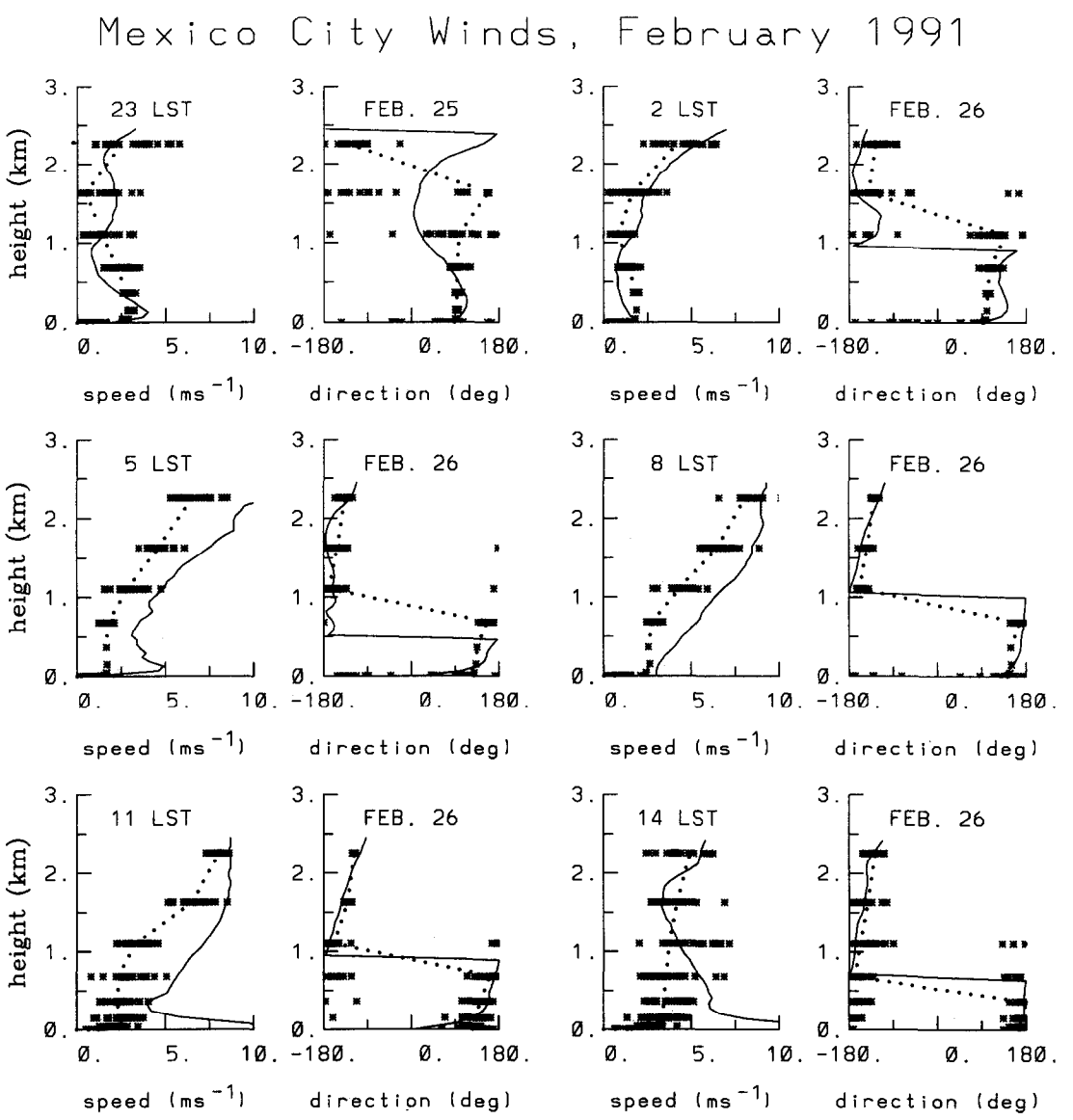

Fig. 13. Comparison of measured wind directions and wind speeds (solid) to modeled mean wind speeds and directions (dotted), and to twenty model realizations (asterisks) for the late hours of 25 February 1991, and the early and midday hours of 26 February 1991.

winds are turning with height, averaging the winds over 250–750 m may artificially reduce the wind speeds.

5. THE DISPERSION MODELING SYSTEM

The dispersion modeling in the Mexico City Air Quality Research Initiative has three objectives: (1) to provide a test of the modeling system against measured data which will provide insight into the transport variables used in the photochemical modeling, (2) to estimate fractional changes in carbon monoxide which cannot be reliably estimated by a linear roll-back because of the changes in the spatial or temporal pattern of emissions, and (3) to estimate the importance of changes in emissions which could effect the SO_2 concentrations in the city.

Dispersion modeling combines the emissions with the meteorology to produce concentrations of non-reactive pollutants. Typically, the dispersion model is asked to represent the average conditions and the high concentrations which occur over a year. It is normally not expected to reproduce the hourly concentrations at the exact positions at which they occur (Bowne, 1981). Small differences between the modeled wind and the actual wind can produce large differences in concentrations from point sources. In the urban context, the situation is somewhat improved because the sources cover a large area and tend to be

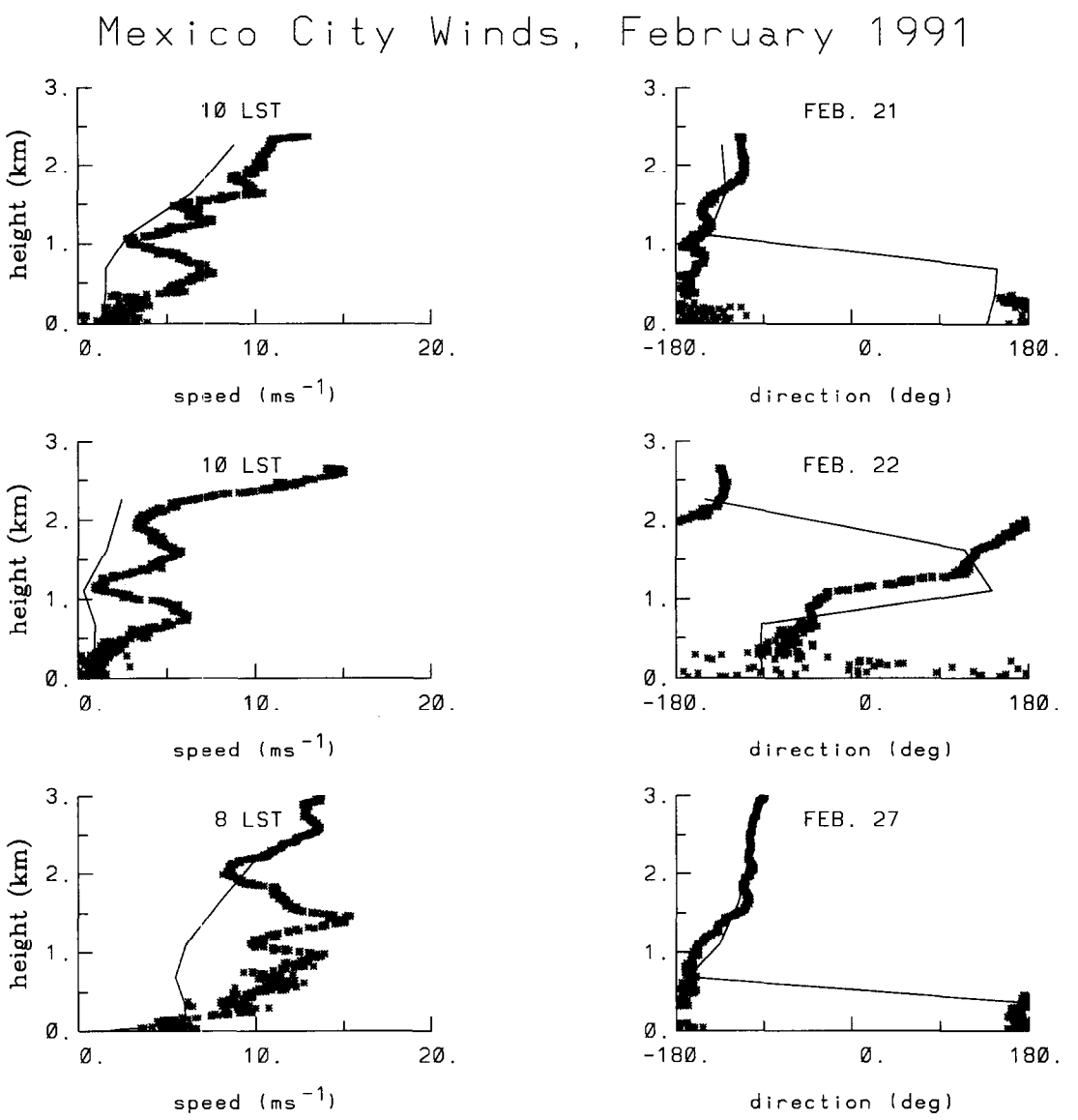

Fig. 14. Comparison of the aircraft measured wind direction and wind speed profiles (asterisks) to the modeled wind direction and wind speed profiles (solid) for 21, 22, and 27 February 1991.

more uniformly distributed and thus less sensitive to the wind directions. The sources of emission, however, can be hard to identify and the source strength may vary rapidly in time.

Two pollutants were modeled with the dispersion model: CO and SO_2. CO is produced by low-level sources such as vehicles and small boilers. Measured concentrations can be very sensitive to the presence of local sources near the monitor. SO_2 is produced by low-level sources such as diesel trucks, but it is also produced by industrial sources such as power plants. Sources which emit contaminants from tall stacks are difficult to model precisely because small changes in wind directions or conditions which affect the plume rise may produce major changes in concentrations measured at a monitor. In Mexico City the problem is further compounded by the high terrain which can deflect the material to different locations. In some instances, models endorsed by the USEPA have failed to display a positive correlation with hour by hour and site by site measurements (Weil and Brower, 1982). However, the models usually show approximately correct peak concentrations and average concentrations and are thus appropriate for air quality planning purposes.

5.1. *Description of the dispersion model*

The RAPTAD dispersion model is a Monte Carlo dispersion and transport code (Yamada and Bunker, 1988). Pseudo-particles are transported with instant-

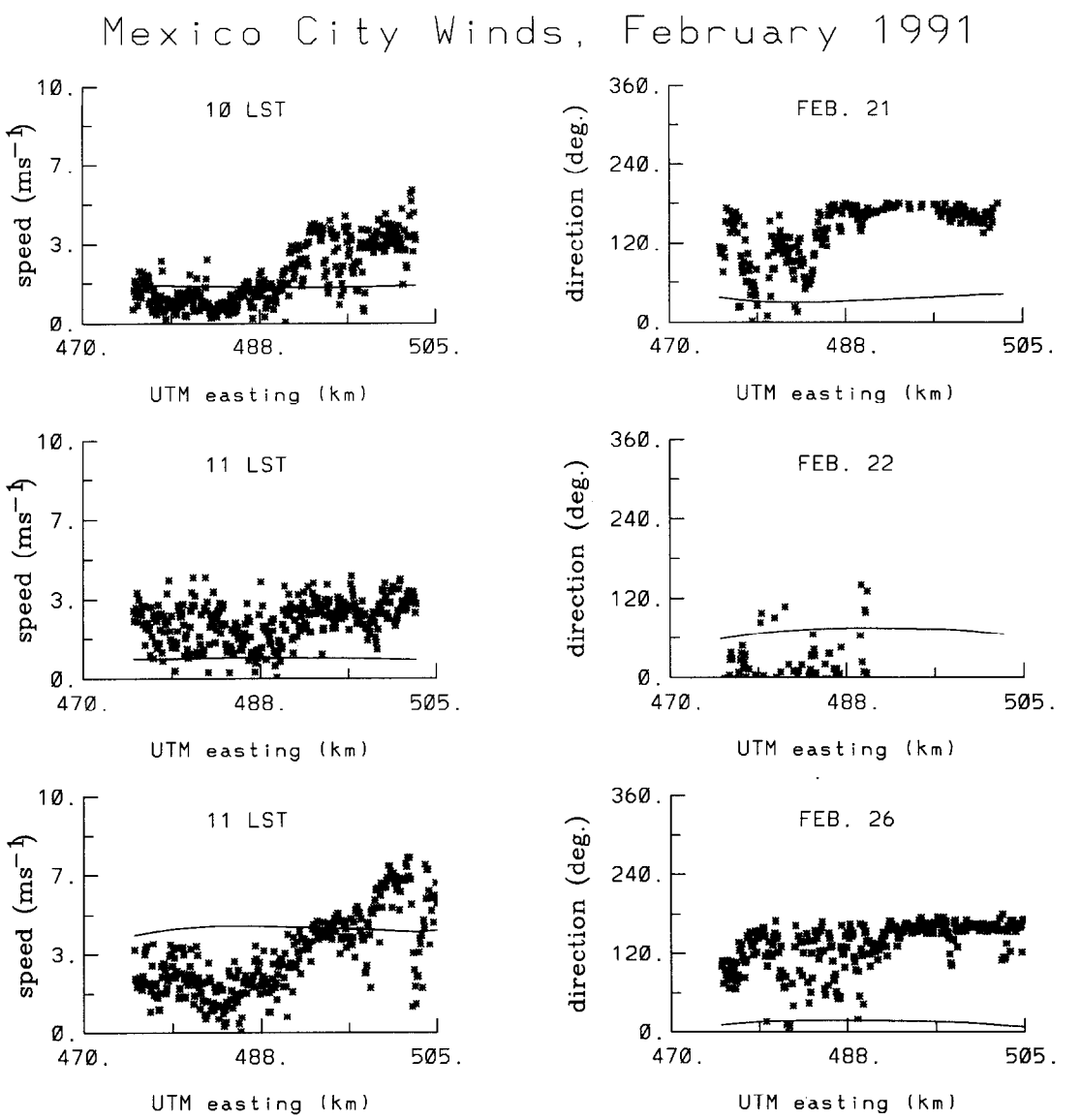

Fig. 15. Comparison of the aircraft measured wind directions and wind speeds (asterisks) on a west to east pass of the city at 2710 m above sea level to the modeled wind directions and wind speeds (solid) on 21, 22, and 26 February 1991.

aneous velocities that include the mean wind field and the turbulent velocities. The turbulent velocity is generated randomly so that it is consistent with the standard deviation of the wind at the particle location. The location of each pseudo-particle represents the center of mass of a concentration distribution for each puff. The total concentration at any point is obtained by adding the concentration contributions from each puff (a kernel method). The Monte Carlo kernel method requires that a functional form for the distribution kernel be chosen and that parameters that describe the width, breadth, and depth of the distribution be calculated. The approach used here is to assume a Gaussian distribution where variances are determined from the time integration of the velocity variances encountered over the history of the puff. The variances are estimated based on the random force theory of turbulent diffusion (Lee and Stone, 1982).

Figure 18 illustrates an application in which these modeling capabilities are essential. The picture illustrates the behavior of the emissions as they leave a refinery and travel toward Mexico City during the night. The globes represent pseudo-particles and the size of the globes is proportional to the vertical standard deviation of the contamination distribution associated with the pseudo-particle. Each pseudo-particle contains the same mass of sulfur dioxide, but different pseudo-particles may have more or less ambient air. The small, blue globes represent pollutant

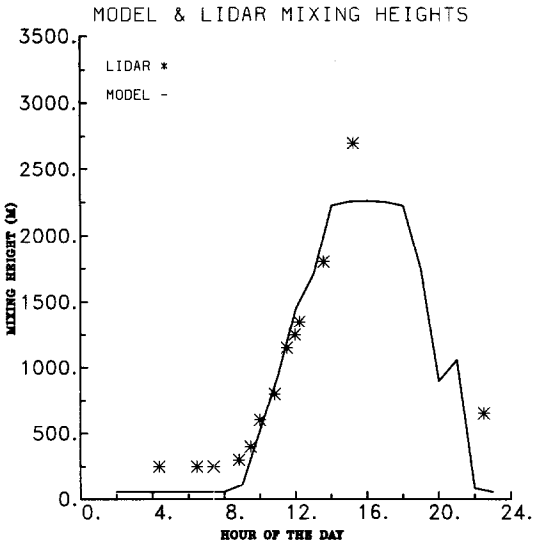

Fig. 16. Comparison of the LIDAR measured mixing heights (asterisks) to the modeled mixing heights (line) for 22 February 1991.

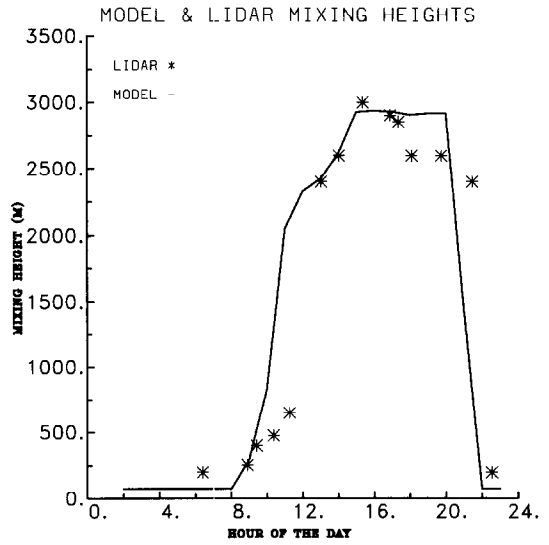

Fig. 17. Comparison of the LIDAR measured mixing heights (asterisks) to the modeled mixing heights (line) for 26 February 1991.

parcels which have high concentrations and small vertical extent. The red globes have more dilute concentrations and a greater vertical spread. Figure 18 shows that the plume remains aloft until it reaches Pico de Tres Padres when some of it is trapped in the drainage air and carried to the surface. The highest one hour concentrations were calculated for site N (San Agustin) and were associated with interaction between the plume and Pico de Tres Padres during the nighttime hours. These simulations were particularly interesting because they pointed to the significance of a situation which has received little attention to date, i.e. elevated flow toward a mountain with subsequent entrapment in the drainage flow and transport to the lowlands. There is no other way to model these circumstances without a model with similar capability.

5.2. *Model development*

Initially, the dispersion model had several limitations: (1) the puff growth was based on a simplistic model which was inappropriate for rapidly changing turbulence conditions, (2) emission rates did not vary over the day, (3) only one source was treated, (4) the plume rise was treated simplistically, and (5) the effect of vertical variations in stability was not reflected in the size of the particle kernel.

These limitations are important because: (1) turbulence can change very rapidly shortly after sunrise, or when a layer aloft is captured by a growing mixed layer, (2) variable emission rates are very important for mobile sources, (3) there are many types of sources which contribute to air quality in Mexico City, (4) the contribution of industrial sources with large boilers to the air quality depends upon the heights obtained through buoyant plume rise, and finally, (5) the volume which is calculated to surround a pseudo-particle is based on the circumstances experienced by the pseudo-particle. If materials are transported in a mixed layer the turbulence may be quite high, but there may be a stable layer aloft in which there is little turbulence. It is inappropriate to let the pseudo-particle volume extend into the stable layer above.

From the random force theory of turbulent diffusion (Lee and Stone, 1982), we have the following expression for the spread in the lateral direction:

$$\sigma_y^2 = [\sigma_{y0}^2 + 2\sigma_{y0}\,\partial\sigma\,\bar{S} + (\partial\sigma)^2]$$

where

$$\partial\sigma = \sqrt{2}\,\sigma_v\,t_{Ly}\sqrt{\frac{\Delta t}{t_{Ly}} - 1 + \exp\left(-\frac{\Delta t}{t_{Ly}}\right)}.$$

The parameter $\bar{S}$ results from the spatial averaging over the plume width. It is given by:

$$\bar{S} = \frac{2}{\xi^2}(\xi - 1 + \exp(-\xi))$$

with

$$\xi = 3.25\frac{\sigma_{y0}}{L}$$

and the Eulerian length scale L approximated as:

$$L = \frac{\sigma_v}{0.39}\,t_{Ly}.$$

In this formulation, we only concern ourselves with the incremental change to a finite puff with initial spread of σ_{y0} over a single time step Δt during which the turbulence conditions are assumed to be constant.

The standard deviation of the lateral velocity fluctuation is σ_v and the Lagrangian integral timescale is t_{Ly}.

The model was modified to use hourly emission rates. It was also modified to permit a large number of sources with each source emitting pseudo-particles in proportion to its fraction of the total emissions from a category, such as all automobiles. Different categories are modeled with separate runs and the results of individual runs were combined to give the total concentrations at each receptor.

The original plume rise description covered only neutral and stable conditions. In the revised model, a considerable improvement of the plume-rise formulations has been developed based on Briggs' work (1984). The model now includes two different treatments for stable conditions, a treatment for elevated inversion layers aloft, a convective turbulence treatment, and two neutral stability treatments. The smallest applicable plume rise is picked as the limiting condition in each case. The plume rise is still based on bulk properties of the atmosphere and does not make full use of the meteorological model outputs which are available.

In the original version of the model the kernel growth was based only on the turbulence experienced by the center of mass of the pseudo-particles. The center of mass of the pseudo-particle released at the surface in a well-mixed layer will tend to travel within the layer and not experience the more stable layers aloft. Consequently, the calculated vertical spread parameter might be too large if there is a strong inversion layer aloft. This concern was addressed by limiting the growth of the vertical spread of particles in the mixed layer to be less than the height of the mixed layer. In cases where the mixed-layer height limits the vertical spread of the kernel, the model uses a vertically uniform distribution instead of a Gaussian distribution. This treatment is very similar to that used by Gaussian puff models except that we are using it for individual pseudo-particle kernels rather than the plume.

One problem with this approach is how to calculate the mixed-layer height based on the HOTMAC meteorological outputs. Fortunately, the suite of models is an ideal one to test an old formulation or to develop and test a new formulation. We examined the potential temperature formulation which defines the mixing height as the height at which the potential temperature is equal to the potential temperature near the surface. We released particles near the surface and plotted their heights and we also plotted the mixing heights based on the potential temperature formulation. Ideally the calculated mixing heights should represent the upper limit of the particle positions. We found that the potential temperature representation greatly overestimated the height of the mixing layer.

Next, we considered a formulation in which we defined the mixing height by the height at which the fluctuations in the vertical velocity, σ_w, dropped below some specified level. This system tended to do a much better job for the mid-morning through afternoon heights, but it sometimes had difficulties with early morning situations. We remedied this defect by defining the mixing height in the early morning by the height at which the vertical potential temperature gradient first became positive. Later in the day we used the σ_w formulation. In the early morning, relatively small values of σ_w are adequate to transport material upward across the thin mixed layers, however, in the afternoon, large values of σ_w are required to disperse the material across the deep mixed layers. Figure 19 displays the particle positions on the fine grid as seen from above at 11 a.m. from an early morning release on 22 February. The bounding lines show what will be displayed in the vertical position plots. The particles which are displayed in Fig. 20 are those which are found between easting coordinates (UTMX) 480 and 500 km. The various lines in Fig. 20 correspond to the mixing height calculated using our new formulation from the various meteorological grids which fall within the UTMY lines. The heights show an increase over higher terrain. For example note the bump in Fig. 20 at UTMY 2165 which corresponds to Pico de Tres Padres as shown in Fig. 19. The calculated mixing heights may still be a little high, but the normally used potential-temperature formulation gives much higher values.

6. DISPERSION MODEL-MEASUREMENT COMPARISONS

There were principally two data sets available for testing the performance of the dispersion model: (1) National Center for Atmospheric Research (NCAR) aircraft measurements and (2) the SEDESOL surface monitoring results. The aircraft measurements provided information on concentrations and winds throughout the mixed layer and over a wide area which is very important to model verification, while the SEDESOL stations gave the concentrations at the surface. The upper-air measurements are important for validating the model-computed mixed-layer transport which is important in the photochemical model. The photochemistry develops over time so that local surface concentrations are less important than mixed-layer volume-averaged concentrations.

Since the SEDESOL measurements are used to determine the air quality of Mexico City, we have chosen to calculate concentrations at the SEDESOL monitoring sites. Furthermore, the monitoring day chosen by SEDESOL is from 7 p.m. one day until 6 p.m. the next day, hence, the RAPTAD simulations were begun on 20 February at 7 p.m. for the first period and continued until early morning on the 23rd. For the second period, simulations were begun at 7 p.m. on 24 February and continued until early morning on 1 March 1991. In each case, the results of the first day were ignored to allow for model spinup.

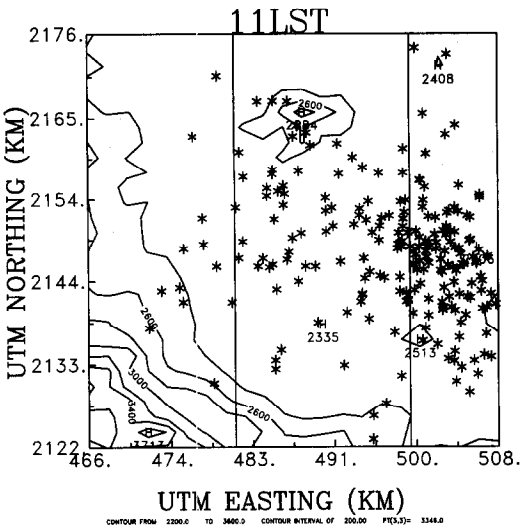

Fig. 19. Calculated pseudo-particle positions displayed on a contour map of the fine grid area for 11 a.m. on 22 February 1991 after an early morning release.

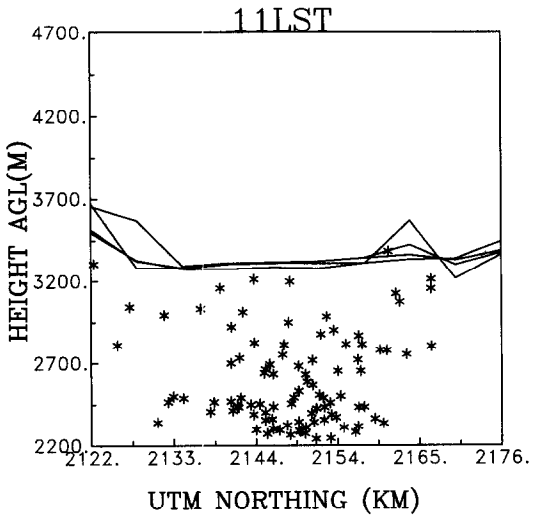

Fig. 20. Calculated vertical positions above ground of pseudo-particles (asterisks) and modeled mixing heights (lines) for all pseudo-particles with UTM easting positions between 480 and 500 km.

6.1. *Aircraft* CO *and* SO_2 *comparisons*

There are two kinds of aircraft measurements which we have used: vertical profiles and horizontal tracings. We have modeled the profiles by calculating the concentrations at intervals of 150 m above the surface up to 1500 m. We have used the coordinates of the airport hangars monitor (station Y) as representative of the profiles, although the aircraft takes off from the runway and climbs out to the northeast. Figure 21 shows the comparison for the airport (solid line) and a point 9 km further east (dashed line) on 22 February 1991. The overpredicted surface concentrations at the airport and the underpredicted surface concentrations east of the airport indicate the horizontal variability of the concentration field. The model does not show the high concentrations aloft found in the measurements. Although both the model computed and lidar measurements yield a mixing height of 500–600 m at 10:00 a.m. on 22 February (see Fig. 16), relatively large CO concentrations are measured up to several km.

Figure 22 shows the comparison for a horizontal traverse from west to east over the center of the city at

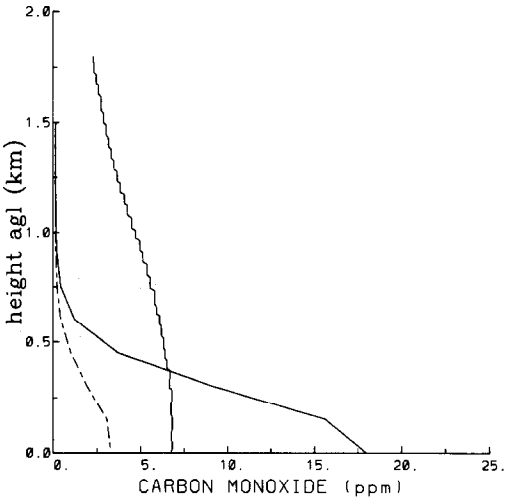

Fig. 21. Comparison of aircraft measured CO concentrations (wavy line) after takeoff from the Mexico city airport with modeled vertical CO profiles from the airport (solid line) and a point 9 km east of the airport (dashed line) for 10 a.m. on 22 February 1991.

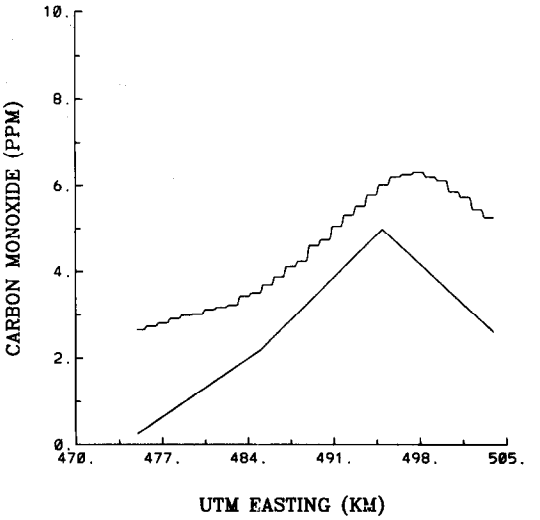

Fig. 22. Comparison of aircraft measured CO concentrations (wavy line) on a west to east traverse of the center of the city to modeled concentrations (line segments) at four points along the traverse for 11 a.m. on 22 February 1991.

500 m above the surface on 22 February. The modeled results are for only four points at Easting coordinates of 475, 485, 495 and 504 km while the Northing coordinate was constant at 2150 km. The measurements and the model show a similar pattern, although the measurements show higher concentrations on either side of the city. The modeled results include no background CO concentrations. A typical background in a remote area would be about 0.2 parts per million, but an appropriate background for Mexico City might be somewhat higher. There are a number of reasons why Mexico City might have a higher background: (1) there is a major city in the basin to the east, Puebla, with smaller cities in the basins to the west, Toluca, south, Cuernavaca, and northeast, Pachuca, (2) smoke is frequently seen from the surrounding forest and agricultural lands, and (3) the basin tends to have a pattern which permits recirculation of the pollutants. While low-level winds are frequently from the northeast the upper-level winds are from the southwest, so that material moves across the basin towards the mountains to the southwest. As the upslope winds develop the material is carried into the southwesterly winds aloft and brought back across the basin where convection mixes it throughout the mixed layer. To the extent that these processes occur within the modeling domain it should be captured by the model if the simulations are continued sufficiently long. However, material that is mixed down and then captured by the slope winds which originate near the Gulf would not be described with the two-grid simulations. If a background concentration of 2.5 ppm were to be added to the modeled results, the agreement between the measurements and the model would be much better.

Figure 23 shows the vertical profile comparison for SO_2 at the airport on 22 February 1991. The model shows a similar pattern, but the concentrations are slightly underestimated. An earlier version of the SO_2 inventory gave a significant overestimate for the modeled profiles. The differences between the two inventories have not been resolved, although the more recent inventory should have better information. However, the newer inventory also includes the effects of more recent control measures which were not yet in place in February 1991. An important deficiency of both inventories is that representative stack parameters are not available for point sources other than the major powerplants and oil refineries. The estimated plume-rise parameters used in the model runs probably do not reflect reality for many stationary sources. Once again, a background concentration of 0.015 ppm would improve the agreement between the model results and the measurements.

Figure 24 shows the SO_2 comparison for a horizontal traverse from west to east over the center of the city at 500 m above the surface on February 22. The modeled results are for only four points at Easting coordinates of 475, 485, 495, and 504. The measurements and the model show a similar pattern, although

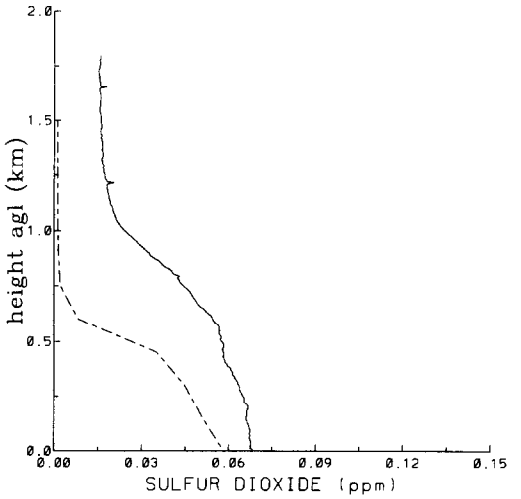

Fig. 23. Comparison of aircraft measured SO_2 concentrations after takeoff from the Mexico city airport with modeled vertical SO_2 profiles (dashed line) from the airport for 10 a.m. on 22 February 1991.

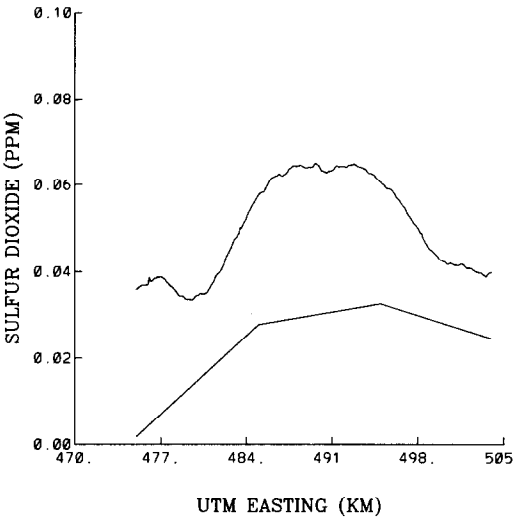

Fig. 24. Comparison of aircraft measured SO_2 concentrations (wavy line) on a west to east traverse of the center of the city to modeled concentrations (line segments) at four points along the traverse for 11 a.m. on 22 February 1991.

the measurements show higher concentrations on either side of the city. The modeled results include no background SO_2 concentrations. In most cases the measured concentrations are low and the model underestimates the observations. Once again the earlier inventory gave much higher modeled values.

6.2. *Surface* CO *and* SO_2 *comparisons*

Figure 25 reports the model-measurement comparison for CO for 22 February 1991. Figure 26 shows the CO comparisons for 28 February. Generally, the model appears to show the correct behavior although

there are cases when the model misses a peak or shows one that should not be there. There are also some cases where the measurements show strange behavior. For example, stations P and O show relatively high concentrations at all times. There has been concern that the stations have a 2.5 ppm offset to avoid processing problems associated with negative concentrations, however, these stations do not seem to all have the same offset. If there is a background of about 2.5 ppm, consistent with the aircraft measurements, the agreement between the modeled results and the surface and aircraft measurements would be much better.

Figure 27 reports the comparison between modeled and measured SO_2 on 22 February 1991. Figure 28 reports a similar comparison for 28 February. Again the model behavior is similar to the measurements. Of particular interest is the difference between Fig. 25 for CO and Fig. 27 for SO_2. Figure 27 depicts early morning peaks in both the model (stations H, E, and L) and the measured results (stations L, J, E, X, and Y) which are not reflected in the CO comparisons. These could be the result of mixing down of plumes aloft in the presence of terrain. Peaks are also seen between 7 a.m. and noon when the low-level emissions are high and when high-level emissions can be mixed down to the surface in the mixed layer.

7. DISPERSION MODEL PERFORMANCE SUMMARY

In Section 4, we listed statistical measures for evaluating model performance. Consequently, we used the same measures even though these measures are likely to provide a somewhat more pessimistic view of model performance. Table 2 summarizes the statistics for the comparison between modeled and measured CO and SO_2 concentrations.

The modeled mean CO concentration is somewhat lower than the observed mean, although a 2.5 ppm instrument-offset correction would give perfect agreement. Generally, the model seems to be doing quite well for CO given the uncertainty in both the emission and meteorological inputs. The model describes the mean and maximum concentrations very well. The regression and correlation coefficients are low, but it is difficult to obtain good hour by hour and station by station agreement in these circumstances. For SO_2, the agreement is not as good and the differences between the results from the two inventories highlight the importance of good inventories. The additions of backgrounds of 2.5 ppm for CO and 0.015 ppm for SO_2 would also produce better agreement between the model and the measurements.

The aircraft measurements suggest pretty good performance overall. However, it is clear that any particular station may not be represented perfectly at any given time. The ambient concentrations tend to support the suggestion in the wind comparisons that there is stronger convergence over the city than the model is producing. The horizontal traverses cast doubt on the proposition that the model is greatly overpredicting the late-morning mixing height.

8. POTENTIAL IMPROVEMENTS

There are a number of areas in which the meteorological modeling could be improved. First, if a domain were drawn which included the Gulf coast, the effects of slope winds which originate near the coast could be better represented. This would be done by surrounding the existing coarse grid with another grid with 18 km cell size. This would allow a better representation of moisture and temperature changes which occur over the course of the simulation and it allows

Table 2. Statistical comparison of modeled and measured CO and SO_2 concentration

Parameter	SO_2 (ppm) old inventory	SO_2 (ppm) new inventory	CO (ppm)
Model mean	0.040	0.017	4.3
Observation mean	0.050	0.050	6.8
Standard deviation of predictions	0.033	0.015	4.2
Standard deviation of observations	0.031	0.031	3.6
Regression intercept	0.033	0.013	1.8
Regression coefficeint	0.15	0.083	0.38
Correlation coefficient	0.14	0.17	0.33
Root-mean-square error	0.043	0.046	5.2
Systematic root-mean-square rror	0.028	0.044	3.4
Unsystematic root-mean-square error	0.032	0.015	3.9
Index of agreement	0.47	0.43	0.55
Skill error	1.0	0.48	1.1
Skill variance	1.1	0.49	1.1
Model maximum	0.27	0.098	30.2
Observation maximum	0.28	0.28	31.5

a better representation of the recirculation of pollutants between the basin and the Gulf coast. Some of the anomalous winds as represented by Station B might be associated with an eddy produced by the effects of the sea-breeze. In the current simulations the effects of the sea breeze were captured by the Tethersonde or rawinsonde driving winds. An additional grid would cost very little in computational time, because the large grid cells would use much longer time steps than those used for the inner grids.

Second, a substantial improvement could be gained by using hourly-averaged winds from the big SODAR now operating in downtown Mexico City. These winds would provide a better representation of the averaged winds which the model uses. This step would require very little or no changes in the model itself.

Third, one could account for the effects of spiralling winds with height and make appropriate adjustments so that wind speeds are not underestimated because of the changes of direction with height. Fourth, one could improve the properties of the surface coverages used in the model. We are currently using bulk properties, which ignore the effects of differences in materials. For example, a small layer of dead vegetation can act as an effective insulator which can produce a much different energy balance. The surface parameters used for various surface coverages represent, at best, preliminary estimates which could probably be significantly improved.

Fifth, the model could be (and subsequently has been) improved by using a better treatment of long-wave radiation. The treatment depends upon a simple representation of how moisture and CO_2 absorb and reradiate energy throughout the atmosphere as a function of temperature. One study (Oke *et al.*, 1992), has measured long-wave radiation about 10% lower than that calculated by the model. The current set of parameters are slightly in error and could be (and subsequently have been) improved. Such changes have a significant effect on the energy balance and do explain why the modeled temperature in the early morning is higher than the measured temperature.

Finally, an improved treatment of the short-wave and long-wave radiation effects of clouds could be incorporated into the model. An improved treatment of short-wave radiation has been tested in a one-dimensional version of the code, but it has not been implemented in the three-dimensional version. The long-wave radiation effects have been used in other applications, but they were not used in this study.

The dispersion modeling could be improved with better emission inventories. Specifically, the current estimates use area sources for the mobile categories, while line sources would improve the spatial resolution. In the context of SO_2 modeling, a good description of the stack parameters for several of the larger sources would be helpful.

REFERENCES

Bowne N. E. (1981) Preliminary Results from the EPRI Plume Model Validation Project-Plains Site. EPRI EA-1788-SY, Electric Power Research Institute.

Briggs G. A. (1984) Plume rise and buoyancy effects. In *Atmospheric Science and Power Production* (edited by Randerson D.), U.S. Dept. of Energy, DOE/TIC -27601, pp. 327–366.

Gertler A. W. and Pierson W. R. (1991) Motor Vehicle Modeling Issues. Paper 91-88.8 in Proceedings Volume 7, Air Modeling Papers from the 84th Annual Meeting, published by the Air & Waste Management Association, Pittsburgh, Pennsylvania.

Lee J. T. and Stone G. L. (1982) The Use of Eulerian Initial Conditions in a Lagrangian Model of Turbulent Diffusion. Los Alamos National Laboratory, LA-UR-82-3034, Los Alamos, New Mexico.

Mardia K. V. (1972) *Statistics of Directional Data*, pp. 127–128. Academic Press Inc., Orlando, Florida.

Oke T. R., Zeuner G. and Jauregi E. (1992) The surface energy balance in Mexico City. *Atmospheric Environment* **26B**, 433–444.

Oliver W. R., Dickson R. J. and Bruckman L. (1993) Development of the SCAQS High-Resolution Emissions Inventory: Assessment of Inventory Uncertainties. In Proc. Int. Specialty Conf., Southern California Air Quality Study, Data Analysis, pp. 62–73. VIP-26 published by the Air & Waste Management Association, Pittsburgh, Pennsylvania.

Tesche T. W., Georgopoulus P., Seinfeld J. H., Cass G., Lurmann F. L. and Roth P. M. (1990) Improvement of Procedures for Evaluating Photochemical Models. Final report contract No. A832-103, prepared for the California Air Resources Board, Radian Corporation, DCN: 90-264-069-05-02.

Thomson D. W. (1986) Systems for measurements at the surface. In *Mesoscale Meteorology and Forecasting* (edited by Ray P.), pp. 71–84. AMS, Boston.

Weil J. C. and Brower R. P. (1982) The Maryland PPSP Dispersion Model for Tall Stacks. PPSP-MP-36, Martin Marietta Corporation, Baltimore, Maryland.

Wilson R. B. (1993) Review of development and application of CRSTER and MPTER models. *Atmospheric Environment* **27B**, 41–57.

Yamada T. (1982) A numerical study of turbulent airflow in and above a forest canopy. *J. Meteor. Soc. Japan* **60**, 111–126.

Yamada T. and Bunker S. (1988) Development of a nested grid, second moment turbulence closure model and application to the 1982 ASCOT Brush Creek data simulation. *J. appl. Met.* **27**, 562–578.